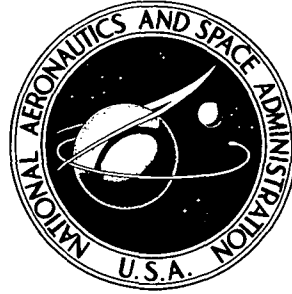


**NASA CONTRACTOR  
REPORT**



*N73-16522*  
NASA CR-2195

NASA CR-2195

**EFFECT OF SURFACE ASPERITY  
ON ELASTOHYDRODYNAMIC LUBRICATION**

*by Kwan Lee and H. S. Cheng*

*Prepared by*  
NORTHWESTERN UNIVERSITY  
Evanston, Ill.  
*for Lewis Research Center*

NATIONAL AERONAUTICS AND SPACE ADMINISTRATION • WASHINGTON, D. C. • FEBRUARY 1973

FILED  
SEP 11 1973  
CSC



1. Report No. NASA CR-2195		2. Government Accession No.		3. Recipient's Catalog No.	
4. Title and Subtitle EFFECT OF SURFACE ASPERITY ON ELASTOHYDRODYNAMIC LUBRICATION				5. Report Date February 1973	
				6. Performing Organization Code	
7. Author(s) Kwan Lee and H. S. Cheng				8. Performing Organization Report No. None	
9. Performing Organization Name and Address Northwestern University Evanston, Illinois				10. Work Unit No.	
				11. Contract or Grant No. NGL-14-007-084	
12. Sponsoring Agency Name and Address National Aeronautics and Space Administration Washington, D.C. 20546				13. Type of Report and Period Covered Contractor Report	
				14. Sponsoring Agency Code	
15. Supplementary Notes Project Manager, Erwin V. Zaretsky, Fluid System Components Division, NASA Lewis Research Center, Cleveland, Ohio					
16. Abstract The important aspects of elastohydrodynamic lubrication, with a single, one-dimensional asperity, have been found by solving numerically the coupled transient Reynolds equation and the elasticity equation. Even though the assumption of a single asperity is highly ideal, this study sheds some light on the effect of surface roughness on elastohydrodynamic lubrication. The results show that the film pressure tends to increase more than the steady state pressure, and in particular, the increase in pressure reaches a maximum as the asperity approaches the inlet of the contact region. The asperity height and the pressure increase above the steady state pressure are closely related to each other; the higher the asperity height, the larger the pressure increase. In the pure rolling case, it has been found that a local pressure peak is not developed. However, in the cases of sliding and rolling, a small, local pressure peak is developed on the pressure profile when the asperity moves into the contact region. In general, the overall film thickness profile increases with increasing asperity height, but is not significantly affected by the asperity width. Moreover, the slope of the overall film thickness profile for the transient cases is much greater than the steady state profile, which is approximately constant across the contact width. The increase in the center film thickness also depends upon the width and height of the asperity. Even for the case of an asperity height of $2H_s$ , the center film thickness increases more than 100 percent compared to the steady state center film thickness.					
17. Key Words (Suggested by Author(s)) Elastohydrodynamics Lubrication Asperity interaction Surfaces				18. Distribution Statement Unclassified - unlimited	
19. Security Classif. (of this report) Unclassified		20. Security Classif. (of this page) Unclassified		21. No. of Pages 75	
				22. Price* \$3.00	



# TABLE OF CONTENTS

	Page
CHAPTER 1 - INTRODUCTION	
1.1 Introduction . . . . .	1
CHAPTER 2 - MATHEMATICAL FORMULATION	
2.1 Introduction . . . . .	3
2.2 Geometry of Asperity . . . . .	4
2.3 Governing Equations . . . . .	4
2.3.1 Film Thickness . . . . .	4
2.3.2 Hydrodynamic Equation . . . . .	6
2.4 Viscosity and Density Variations . . . . .	10
2.5 Formulation of Elastohydrodynamic Problem . . . . .	10
2.5.1 Coupled Time-Dependent Elastohydrodynamic Equations . . . . .	10
2.5.2 Normalization . . . . .	12
2.6 Method of Solution . . . . .	14
2.6.1 Outline of Approach . . . . .	14
2.6.2 Integration of Pressure in the Inlet Pressure . . . . .	15
2.6.3 Calculation of Deformation . . . . .	16
2.6.4 Elastohydrodynamic Equation in the Middle Region . . . . .	18
2.6.5 Calculation of Center Film Thickness . . . . .	21
2.6.6 Outline of Numerical Procedure . . . . .	22
CHAPTER 3 - DISCUSSION OF RESULTS	
3.1 Introduction . . . . .	25
3.2 Pressure Profile . . . . .	25
3.3 Film Thickness . . . . .	27
3.4 Load . . . . .	29
CHAPTER 4 - SUMMARY OF RESULTS . . . . .	30
APPENDIX A - Symbols List . . . . .	45
APPENDIX B - Calculation of Matrix Elements in Eq. (51) . . . . .	50
APPENDIX C - Computer Program Flow Diagram and Fortran Listings . . . . .	55
REFERENCES . . . . .	74



# CHAPTER I

## INTRODUCTION

### 1.1 INTRODUCTION

Since Reynold developed the hydrodynamic lubrications theory, bearing performance between two parallel or two conformable surfaces can be readily determined by solving the Reynolds equation for the pressure distribution within the lubricant film. However, for highly loaded, counterformed contacts such as ball, roller, or gear tooth contacts, it was found that hydrodynamic theory alone cannot explain the lubrication phenomenon. The film thickness obtained from the hydrodynamic equation is so small that direct metallic contacts between asperities must take place and cause surface distress. However, in practice, these concentrated contacts do operate quite satisfactorily without any signs of distress in lubrication. This indicates strongly that some degrees of hydrodynamic lubrication must exist between these counterformal contacts. The analytical proof of the surface separation between these contacts was first given by Grubin [1] by including the surface deformation and the effect of a variable viscosity. His work opened a new branch of lubrication known as elastohydrodynamic lubrication.

During the past two decades, rapid progress has been made in elastohydrodynamic lubrication. There now exist several numerical solutions to determine the pressure and film thickness profiles [2 to 5]. Also available are simplified formulas to compute the minimum film thickness in terms of load, speed, and lubricant parameters. However, in all



these EHD theories, the contacting surfaces are assumed to be perfectly smooth. In reality, surfaces are never perfectly smooth, and for conditions where the average height of the asperities approaches or exceeds the mean film thickness, the smooth-film elastohydrodynamic theories are no longer valid. The asperities can have a significant influence upon the pressure and film thickness profiles. To determine the interaction between the lubricant and asperities, it is necessary to solve the transient elastohydrodynamic equations as the asperities moving through the contact region.

The present study concentrates on the interaction of a single asperity with lubricant as it enters the inlet region of an elastohydrodynamic contact. By solving the coupled elasticity and hydrodynamic equations at successive time intervals during the entrance of a single asperity, the modification of the pressure distribution and the film thickness level around the asperity can be determined.



## CHAPTER II

### MATHEMATICAL FORMULATION

#### 2.1 Introduction

Due to the presence of the asperity on the moving surface, both the pressure and film deformation become time-dependent as the asperity enters the contact region. To determine the change in pressure and deformation caused by the asperity, it is required to solve the coupled elastohydrodynamic equation at successive time intervals taking into account the effect of the squeeze film term. For each time interval, the effort required for determining the pressure and deformation profile is equivalent to a single, conventional, elastohydrodynamic solution.

For heavily loaded contacts, the conventional EHD theories show that the pressure and deformation profiles in the central region of the contact are almost identical to the dry-contact, Hertzian profiles. Deviations from Hertzian distributions only occur at the inlet and exit regions. This fact enables one to investigate the effect of asperity in the inlet and exit regions separately. It is assumed that the disturbance caused by the asperity at the inlet region is not felt in the exit region and vice versa.

The present study is primarily concerned with the effect of the asperity in the inlet region. In solving the time-dependent EHD equations, the pressure distribution in the exit-half of the contact region is assumed to be the Hertzian elliptical distribution.



## 2.2 Geometry of Asperity

The surface geometry adopted in the present study is the perfectly smooth contact surface of the cylinder attached with a single, one-dimensional asperity of parabolic shape as shown in Fig. 1. In the present study, the height and the width of asperity are changed in such a way that each effect can be investigated separately. The maximum values of height and width of the asperity are twice the center film thickness and one-half of the Hertzian width of the same center pressure. The average of the rolling speeds of the two cylinders is kept constant which in turn fixes the center film thickness of the steady state solution with a fixed center pressure.

## 2.3 Governing Equations

### 2.3.1 Film Thickness

The geometrical configuration of two cylinders can be shown to be equivalent to a cylinder and a flat surface as shown on Fig. 1(c). The radius of the equivalent cylinder is

$$R = \frac{R_1 + R_2}{\frac{R_1 R_2}{R_1 + R_2}} \quad (1)$$

Since the contact region is much smaller compared to the radius of the cylinder, the geometrical film thickness without the height of the asperity is,

$$h_g = h'_o + \frac{x^2}{2R} \quad (2)$$



The height of the asperity is approximated by the parabolic equation as

$$f = f_1 \cos \theta = \frac{1}{2r} \left[ (x_3 - x)^2 - c_4^2 \right] \cos \theta \quad (3)$$

Because of the narrowness of the contact width,  $\cos \theta \approx 1.0$ .

It follows that the asperity height can be approximated by,

$$f \approx f_1 = \frac{1}{2r} \left[ (x_3 - x)^2 - c_4^2 \right] \quad (4)$$

Thus, the geometrical film thickness with the asperity height is,

$$h_g = h'_0 + \frac{x^2}{2R} + \frac{1}{2r} \left[ (x_3 - x)^2 - c_4^2 \right] \quad (5)$$

The deformation of the contact surfaces, as derived in Ref. [6].

$$d(x, t) = - \frac{4}{\pi E} \int_{-\infty}^{\infty} P(\xi, t) \ln \frac{|\xi - x|}{|\xi|} d\xi \quad (6)$$

where

$$\frac{1}{E} = \frac{1}{2} \left( \frac{1 - \nu_1^2}{E_1} + \frac{1 - \nu_2^2}{E_2} \right)$$

and  $E_1$ ,  $E_2$  and  $\nu_1$ ,  $\nu_2$  are the Young's modulus and the Poisson's ratio of the cylinder 1 and 2, respectively.

The film thickness including the deformation becomes

$$\begin{aligned} h(x, t) &= h_0(t) + \frac{x^2}{2R} - \frac{4}{\pi E} \int_{-\infty}^{\infty} P(\xi, t) \ln \frac{|\xi - x|}{|\xi|} d\xi \\ &+ \frac{1}{2r} \left[ (x_3 - x)^2 - c_4^2 \right] \\ &= h_1(x, t) + f \end{aligned} \quad (7)$$



### 2.3.2 Hydrodynamic Equation

In the present study, the transient, one dimensional Reynolds equation is taken as the governing equation for the pressure distribution.

$$\frac{\partial}{\partial x} \left( \frac{\rho h^3}{12\mu} \frac{\partial p}{\partial x} \right) = \frac{u_1 + u_2}{2} \frac{\partial(\rho h)}{\partial x} + \frac{\partial(\rho h)}{\partial t} \quad (8)$$

As mentioned in Section 2.1, the present study is mainly concerned with the first half of the contact region, and the pressure distribution in the second half of the contact region is assumed to be Hertzian. Thus, the appropriate boundary condition is that the center pressure gradient is zero, but the center film thickness is allowed to change as dictated by the pressure distribution in the first half of the contact region.

The boundary conditions for Eq. (8) are

$$\begin{aligned} P &= 0 & \text{at } x &= -\infty \\ \frac{\partial P}{\partial x} &= 0 & \text{at } x &= 0 \end{aligned} \quad (9)$$

#### (a) The Case For Pure Rolling

When the two cylinders are in rolling motion without sliding, the time derivative and the spatial derivative of "f" cancel out each other as shown below:

$$\begin{aligned} \frac{\partial(\rho h)}{\partial t} &= \frac{\partial}{\partial t} \left[ \rho \left( h_o + \frac{x^2}{2R} + d + f \right) \right] \\ &\approx \frac{\partial(\rho h_o)}{\partial t} + f \frac{\partial \rho}{\partial t} + \frac{u}{r} \rho (x_3 - x) \end{aligned} \quad (10)$$



Since the cylinder surfaces are approximately parallel in the contact region, the sum of the cylinder curvature and deformation terms is very small. Furthermore, their time derivative is negligible.

$$\begin{aligned} \frac{u_1 + u_2}{2} \frac{\partial(\rho h)}{\partial x} &= u \frac{\partial}{\partial x} [\rho(h_1 + f)] \\ &= u \frac{\partial(\rho h_1)}{\partial x} + u f \frac{\partial \rho}{\partial x} - \frac{u}{r} \rho(x_3 - x) \end{aligned} \quad (11)$$

In the above manipulations, the following are used:

$$\frac{\partial x_3}{\partial t} = u_1 \quad \text{and} \quad u_1 = u_2 = u$$

the sum of Eq. (10) and (11) is

$$\frac{\partial(\rho h)}{\partial t} + \frac{u_1 + u_2}{2} \frac{\partial(\rho h)}{\partial x} = u \frac{\partial(\rho h_1)}{\partial x} + \frac{\partial(\rho h_o)}{\partial t} + f(u \frac{\partial \rho}{\partial x} + \frac{\partial \rho}{\partial t}) \quad (12)$$

Substituting Eq. (12) into Eq. (8), one obtains

$$\frac{\partial}{\partial x} \left( \frac{\rho h^3}{12\mu} \frac{\partial P}{\partial x} \right) = u \frac{\partial(\rho h_1)}{\partial x} + \frac{\partial(\rho h_o)}{\partial t} + f(u \frac{\partial \rho}{\partial x} + \frac{\partial \rho}{\partial t}) \quad (13)$$

where

$$f(x, x_3) = \frac{1}{2r} \left[ (x_3 - x)^2 - c_4^2 \right] \quad |x_3 - x| \leq c_4$$

$$f(x, x_3) = 0 \quad |x_3 - x| > c_4$$

Eq. (13) is integrated from  $x = -x$  to  $x = 0$  using the second boundary condition of (9).

$$\frac{\partial P}{\partial x} = \frac{12\mu}{\rho h^3} \left\{ u \left( \rho h_1 - \rho h_1 \right) \Big|_{x=0} - \int_{-x}^0 \left[ \frac{\partial(\rho h_o)}{\partial t} + f(u \frac{\partial \rho}{\partial x} + \frac{\partial \rho}{\partial t}) \right] dx \right\} \quad (14)$$



A new variable  $Q$  is introduced to calculate the inlet pressure and the center film thickness. The advantage of using  $Q$  is to eliminate strong dependence of pressure on viscosity in the governing equation. The explicit viscosity term does not appear in the governing equation if the pressure gradient is replaced by the derivative of  $Q$ .

Defining  $Q$  as

$$Q = 1 - \frac{1}{\bar{\mu}} \quad (15)$$

where  $\bar{\mu} = \frac{\mu}{\mu_s}$  and  $\mu_s$  is the ambient viscosity.

The spatial derivative of  $Q$  is

$$\begin{aligned} \frac{\partial Q}{\partial x} &= \frac{1}{\bar{\mu}} \frac{\partial (\ln \bar{\mu})}{\partial P} \frac{\partial P}{\partial x} \\ &= \frac{\alpha}{\bar{\mu}} \frac{\partial P}{\partial x} \end{aligned} \quad (16)$$

The pressure derivative in Eq. (14) is replaced by  $\frac{\partial Q}{\partial x}$ .

$$\frac{\partial Q}{\partial x} = \frac{12\mu_s \alpha}{\rho h^3} \left\{ u \left( \rho h_1 - \rho h_1 \right) \Big|_{x=0} - \int_{-x}^0 \left[ \frac{\partial (\rho h_o)}{\partial t} + f(u) \left( \frac{\partial \rho}{\partial x} + \frac{\partial \rho}{\partial t} \right) \right] dx \right\} \quad (17)$$

Integrating Eq. (17) again from  $x = -\infty$  to  $x$  gives

$$\begin{aligned} Q &= 12\mu_s \alpha \int_{-\infty}^x \left\{ \left( \frac{1}{\rho h^3} \right) \left[ u \left( \rho h_1 - \rho h_1 \right) \Big|_{x=0} - \int_{-x}^0 \left[ \frac{\partial (\rho h_o)}{\partial t} + f(u) \left( \frac{\partial \rho}{\partial \xi} + \right. \right. \right. \right. \\ &\quad \left. \left. \left. + \frac{\partial \rho}{\partial t} \right) \right] d\xi \right] \right\} dx \end{aligned} \quad (18)$$

The above equation will be used in the calculation of the inlet pressure and the center film thickness.



The instantaneous load per unit width of the cylinder is the sum of the integrals of the first half pressure profile and the Hertzian pressure in the second half of the contact region.

$$W(t) = \int_{-\infty}^0 P(x,t) dx + \frac{\pi R P_o^2}{E} \quad (19)$$

(b) The Case For Rolling And Sliding

When the two cylinders undergo a rolling and sliding motion, the time derivative and the spatial derivative of "f" do not cancel out each other as was the case for pure rolling. Thus, the asperity effect on the fluid film becomes much stronger than that of the pure rolling.

The expanded forms of the rolling and squeezing terms are:

$$\frac{\partial(\rho h)}{\partial t} \cong \frac{\partial(\rho h_o)}{\partial t} + f \frac{\partial \rho}{\partial t} + \frac{u_1}{r} (x_3 - x) \quad (20)$$

$$\begin{aligned} \frac{u_1 + u_2}{2} \frac{\partial(\rho h)}{\partial x} &= \frac{u_1 + u_2}{2} \left[ \frac{\partial(\rho h_1)}{\partial x} + \frac{\partial(\rho f)}{\partial x} \right] \\ &= \frac{u_1 + u_2}{2} \left[ \frac{\partial(\rho h_1)}{\partial x} + f \frac{\partial \rho}{\partial x} - \frac{\rho}{r} (x_3 - x) \right] \end{aligned} \quad (21)$$

In Eq. (20) the sum of cylinder curvature and deformation terms is neglected as explained before. Substituting Eq. (20) and (21) into Eq. (8), one obtains

$$\begin{aligned} \frac{\partial}{\partial x} \left( \frac{\rho h^3}{12\mu} \frac{\partial p}{\partial x} \right) &= \frac{u_1 + u_2}{2} \left[ \frac{\partial(\rho h_1)}{\partial x} + f \frac{\partial \rho}{\partial x} \right] + \frac{\partial(\rho h_o)}{\partial t} + f \frac{\partial \rho}{\partial t} \\ &\quad + (u_1 - u_2)(x_3 - x) \frac{\rho}{2r} \end{aligned} \quad (22)$$

where



$$\begin{aligned}
f(x_3, x) &= \frac{1}{2r} \left[ (x_3 - x)^2 - c_4 \right] & |x_3 - x| &\leq c_4 \\
f(x_3, x) &= 0 \\
(u_1 - u_2)(x_3 - x) \frac{\rho}{2r} &= 0 & |x_3 - x| &> c_4
\end{aligned}$$

Eq. (22) is integrated from  $x = -x$  to  $x = 0$  using the second boundary condition of (10). Thus we obtain

$$\begin{aligned}
\frac{\partial P}{\partial x} &= \frac{12\mu}{\rho h^3} \left\{ \frac{u_1 + u_2}{2} \left( \rho h_1 - \rho h_1 \right)_{x=0} - \int_{-x}^0 \left[ \frac{u_1 + u_2}{2} \left( f \frac{\partial \rho}{\partial x} \right) + \frac{\partial(\rho h_o)}{\partial t} \right. \right. \\
&\quad \left. \left. + f \frac{\partial h_o}{\partial t} + (u_1 - u_2)(x_3 - x) \frac{\rho}{2r} \right] dx \right\} \quad (23)
\end{aligned}$$

## 2.4 Viscosity and Density Variations

The property of lubricant is assumed to depend upon pressure only; the viscosity is a exponential function of pressure with a suitable pressure-viscosity coefficient and the density function used in the present investigation is the one developed by Dowson and Whitaker [5].

$$\mu = \mu_s e^{\alpha P} \quad (24)$$

$$\rho = \rho_s \left( 1 + \frac{bP}{1 + a_1 P} \right) \quad (25)$$

where  $\mu_s$  and  $\rho_s$  are the ambient viscosity and density, respectively.

## 2.5 Formulation of Elastohydrodynamic Problem

### 2.5.1 Coupled Time-Dependent Elastohydrodynamic Equations

No previous work has ever undertaken a time-dependent EHD problem of pure rolling or rolling and sliding. The complexity



of the present problem is multiplied by bringing in the asperity action on the fluid film in the contact region. The successful attempt for obtaining the full solution requires not only solving the hydrodynamic equation and the elasticity equation, but also the center film thickness calculation at each instantaneous location of the asperity.

The major equations to be solved are:

(a) The case for pure rolling

$$\frac{\partial P}{\partial x} = \frac{12\mu}{\rho h^3} \left\{ u \left( \rho h_1 - \rho h_1 \right) \Big|_{x=0} - \int_{-x}^0 \left[ \frac{\partial(\rho h_0)}{\partial t} + f(u) \frac{\partial \rho}{\partial x} + \frac{\partial \rho}{\partial t} \right] dx \right\} \quad (14)$$

$$h(x, t) = h_0(t) + \frac{x^2}{2R} - \frac{4}{\pi E} \int_{-\infty}^{\infty} P(\xi, t) \ln \frac{|\xi - x|}{|\xi|} d\xi + f(x, x_3) \quad (7)$$

where

$$f(x, x_3) = \frac{1}{2r} \left[ (x_3 - x)^2 - c_4 \right] \quad |x_3 - x| \leq c_4$$

$$f(x, x_3) = 0 \quad |x_3 - x| > c_4$$

(b) The case for rolling and sliding

$$\begin{aligned} \frac{\partial P}{\partial x} = \frac{12\mu}{\rho h^3} \left\{ \frac{u_1 + u_2}{2} \left( \rho h_1 - \rho h_1 \right) \Big|_{x=0} - \int_{-x}^0 \left[ \frac{u_1 + u_2}{2} \left( f \frac{\partial \rho}{\partial x} \right) + \frac{\partial(\rho h_0)}{\partial t} \right. \right. \\ \left. \left. + f \frac{\partial \rho}{\partial t} + (u_1 - u_2)(x_3 - x) \frac{\rho}{2r} \right] dx \right\} \quad (22) \end{aligned}$$

$$h(x, t) = h_0(t) + \frac{x^2}{2R} - \frac{4}{\pi E} \int_{-\infty}^{\infty} P(\xi, t) \ln \frac{|\xi - x|}{|\xi|} d\xi + f(x, x_3) \quad (7)$$

where



$$\begin{aligned}
f(x, x_3) &= \frac{1}{2r} \left[ (x_3 - x)^2 - c_4^2 \right] & |x_3 - x| \leq c_4 \\
f(x, x_3) &= 0 & \\
(u_1 - u_2)(x_3 - x) \frac{\rho}{2r} &= 0 & \left. \vphantom{\begin{aligned} f(x, x_3) &= 0 \\ (u_1 - u_2)(x_3 - x) \frac{\rho}{2r} &= 0 \end{aligned}} \right\} |x_3 - x| > c_4
\end{aligned}$$

### 2.5.2 Normalization

The following non-dimensional variables are introduced:

$$P = \frac{P}{P_o}, \quad \bar{H} = \frac{h}{h_o}, \quad H_o = \frac{h_o}{R}, \quad X = \frac{x}{a}, \quad Z = \frac{z}{a}, \quad U = \frac{\mu_s u_1}{ER},$$

$$\bar{D} = \frac{d}{h_o}, \quad \bar{f} = \frac{f}{R}, \quad T = \frac{u_1}{a} t, \quad W = \frac{w}{ER}, \quad \bar{\rho} = \frac{\rho}{\rho_s}, \quad \bar{\alpha} = \frac{\alpha}{P_o},$$

$$C_4 = \frac{c_4}{a}, \quad \bar{r} = \frac{r}{R}, \quad P_{Hz} = \frac{P_o}{E}, \quad A_1 = \frac{a_1}{P_o}, \quad B = \frac{b}{P_o}$$

where  $a$  is the Hertzian half-width and the subscript "o" indicates the variables at the film center.

The normalized governing equation are written as:

(a) The case for pure rolling

$$\frac{\partial P}{\partial X} = \left( \frac{48 \mu U}{H_o^2 H} \right) \left\{ \left( \bar{H}_1 - \frac{\bar{\rho}_o}{\bar{\rho}} \right) - \left( \frac{1}{\bar{\rho} H_o} \right) \int_{-x}^0 \left[ \left( \frac{\partial(\bar{\rho} H_o)}{\partial T} + \bar{f} \left( \frac{\partial \bar{\rho}}{\partial X} + \frac{\partial \bar{\rho}}{\partial T} \right) \right) dx \right] \right\} \quad (26)$$

$$\bar{H} = H_1 + \frac{\bar{f}}{H_o} \quad (27)$$

$$H_1 = 1 + \left( \frac{16 P_{Hz}}{H_o \pi} \right)^2 X^2 + \bar{D}(X, T) \quad (28)$$

$$\bar{D}(X, T) = - \left( \frac{16 P_{Hz}}{H_o \pi} \right)^2 \int_{-\infty}^1 P(Z, T) \ln \frac{|Z - X|}{|Z|} dZ \quad (29)$$



$$Q = \frac{48U\bar{\alpha}}{H_o} \int_{-\infty}^x \left\{ \left( \frac{1}{H^3} \right) \left( H_1 - \frac{\bar{\rho}_o}{\bar{\rho}} \right) - \frac{1}{\bar{\rho}H_o H^3} \int_{-x}^o \left[ \frac{\partial(\bar{\rho}H_o)}{\partial T} + \bar{f} \left( \frac{\partial \bar{\rho}}{\partial T} + \frac{\partial \bar{\rho}}{\partial Z} \right) \right] dz \right\} dz \quad (30)$$

where

$$\bar{f} = \left( \frac{8P_{HZ}}{r} \right)^2 \left[ (X_3 - X)^2 - C_4^2 \right] \quad |X_3 - X| \leq C_4$$

$$\bar{f} = 0 \quad |X_3 - X| > C_4$$

(b) The case for rolling and sliding

The rolling speed of the lower cylinder  $u_2$  can be expressed in terms of  $u_1$  with an appropriate coefficient which depends upon a sliding speed desired between the two cylinders.

Let  $u_2 = b_1 u_1$ , and substituting  $b_1 u_1$  in Eq. (22)

$$\frac{\partial P}{\partial X} = \left( \frac{48\bar{\mu}U}{H_o^2 H^3} \right) \left\{ (0.5)(1 + b_1) \left( \bar{H}_1 - \frac{\bar{\rho}_o}{\bar{\rho}} \right) - \frac{1}{\bar{\rho}H_o H^3} \int_{-X}^o \left[ (0.5)(1 + b_1) \left( \bar{f} \frac{\partial \bar{\rho}}{\partial X} + \frac{\partial(\bar{\rho}H_o)}{\partial T} + \bar{f} \frac{\partial \bar{\rho}}{\partial T} + (1 - b_1)(X_3 - X) \left( \frac{8P_{HZ}}{r} \right)^2 \bar{\rho} \right] dx \right\} \quad (31)$$

$$Q = \left( \frac{48U\bar{\alpha}}{H_o^2} \right) \int_{-\infty}^x \left\{ (0.5) \left( \frac{1 + b_1}{H^3} \right) \left( \bar{H}_1 - \frac{\bar{\rho}_o}{\bar{\rho}} \right) - \left( \frac{1}{\bar{\rho}H_o H^3} \right) \int_{-X}^o \left[ (0.5) (1 + b_1) \left( \bar{f} \frac{\partial \bar{\rho}}{\partial X} + \frac{\partial(\bar{\rho}H_o)}{\partial T} + \bar{f} \frac{\partial \bar{\rho}}{\partial T} + (1 - b_1)(X_3 - Z) \left( \frac{8P_{HZ}}{r} \right)^2 \bar{\rho} \right] dz \right\} dx \quad (32)$$

where



$$\bar{f}(x, x_3) = \left( \frac{8P_{HZ}}{r} \right)^2 \left[ (x_3 - x)^2 - c_4^2 \right] \quad |x_3 - x| \leq c_4$$

$$\bar{f}(x, x_3) = 0 \quad |x_3 - x| > c_4$$

The dimensionless load becomes

$$W = 4P_{HZ}^2 \left[ \int_{-\infty}^0 P(X, T) dx + \pi \right] \quad (33)$$

## 2.6 Method of Solution

### 2.6.1 Outline of Approach

Since the pressure profile in the second half of the contact region is assumed to be the Hertzian pressure profile, the solutions for the first half pressure and film thickness profiles are obtained in the present study. The first half of the contact region is divided into two regions - the inlet and middle region.

The increase in the inlet pressure is gradual and does not reach a high value comparing with the pressure in the middle region. Thus, the nonlinearity of the governing equation is not severe, and consequently the direct iteration method can be used for the calculation of inlet pressure without introducing any convergence difficulty. Rather than calculating pressure directly from the governing equation,  $Q$  is obtained first by Eq. (30) for pure rolling case or Eq. (32) for rolling and sliding case. Then, from  $Q$  the inlet pressure is obtained.

In the middle region, the system equations in the finite difference form are solved by the Newton-Raphson method. The solution



of the system equations gives the pressure correction terms at every grid point in the middle region. Since finer grid spacings are required near the asperity to account accurately the variation of pressure and film thickness around the asperity, it is necessary to change the grid spacings for successive time intervals as the asperity moves toward the center. Thus, at each time interval, the previous values of pressure, film thickness and density are determined by linear interpolation to use in the calculation of time derivatives of these variables. Details of numerical treatment for the pressure and film thickness profiles and the center film thickness will be given in the next section.

### 2.6.2 Integration of Pressure in the Inlet Region

The equation used for inlet pressure calculation is written at Kth grid point and time  $T_m$ :

$$Q_{K,m} = \left( \frac{48U\bar{\alpha}}{H_o^2} \right)_m \int_{-\infty}^{X_K} \left\{ \left( \frac{1}{H_m^3} \right) \left( H_{1m} - \frac{\bar{p}_o}{\bar{\rho}_m} \right) - \left( \frac{1}{\bar{\rho}_o H_m^3} \right)_m \int_{-X}^{\infty} \left[ \frac{\partial(\bar{\rho} H_o)}{\partial T} \right. \right. \\ \left. \left. + \bar{f} \left( \frac{\partial \bar{p}}{\partial T} + \frac{\partial \bar{p}}{\partial Z} \right) \right]_m dZ \right\} dX = (U_1)(\phi_K) \quad (30)$$

where

$$U_1 = \left( \frac{48U\bar{\alpha}}{H_o^2} \right)_m$$

In evaluating the integral in Eq. (30), the pressure, density and deformation are considered to be known and are taken as the previously iterated values.



Defining  $-x_{KA}$  as the dividing point between the inlet and middle region,  $Q_{KA,m}$  can be written as

$$Q_{KA,m} = (U_1)(\phi_{KA})$$

From the above equation

$$U_1 = \frac{Q_{KA,m}}{\phi_{KA}} \quad (34)$$

Substituting Eq. (34) for  $U_1$  into Eq. (30), one can eliminate  $U_1$  in Eq. (30)

$$Q_{K,m} = (Q_{KA,m})\left(\frac{\phi_K}{\phi_{KA}}\right) \quad (35)$$

where  $Q_{KA,m}$  is determined by the solution of the system equation in the middle region. Once  $Q_{K,m}$  is determined, through Eq. (15)  $P_{K,m}$  is obtained.

For the case of rolling and sliding, Eq. (32) is used to obtain the inlet pressure following the same method described above.

### 2.6.3 Calculation of Deformation

The numerical quadrature for the singular kernel in Eq. (30) is the same as the one detailed in Section 2.5.3 in Part I. However, the upper limit of the deformation integral in Part II differs from that of Part I. The pressure distribution in the second half of the contact region is the Hertzian profile and the width of it is also the Hertzian half-width  $a$ .



$$\int_{-X_{KI}}^1 P_m(z) \ln |z - X_K| dz = \sum_{j=1,3,5}^{Kf-2} \left[ P_{j,m}^{K_1}(-X_K, -Z_j) + P_{j+1,m}^{K_2}(-X_K, -Z_j) + P_{j+2,m}^{K_3}(-X_K, -Z_j) \right] \quad (36)$$

$$\int_{-KI}^1 P_m(z) \ln |z| dz = \sum_{j=1,3,5}^{Kf-2} \left[ P_{j,m}^{K_1}(-X_{K0}, -Z_j) + P_{j+1,m}^{K_2}(-X_{K0}, -Z_j) + P_{j+2,m}^{K_3}(-X_{K0}, -Z_j) \right] \quad (37)$$

where  $K_1$ ,  $K_2$  and  $K_3$  were defined by Eq. (42), (43) and (44) of Ref. 6, and  $X_{Kf}$  is unity. When  $Z_j$  is larger than  $Z_{K0}$ ,  $-Z_j$  is replaced by  $Z_j$  in Eq. (42), (43) and (44) of Ref. 6.

In order to facilitate the differentiation  $P_{K,m}$  with respect to  $P_{j,m}$ ,  $K_1$ ,  $K_2$  and  $K_3$  are rearranged in such a way that  $P_{j,m}$  has a single coefficient  $R(-X_K, -Z_j)$ :

$$\begin{aligned} R(-X_K, Z_j) &= S_1(-X_K, -Z_j) & j &= 1 \\ &= S_2(-X_K, -Z_{j-1}) & \text{even } 2 \leq j \leq Kf-1 \\ &= S_3(-X_K, -Z_{j-2}) + S_1(-X_K, -Z_j) & \text{odd } 3 \leq j \leq Kf-2 \\ &= S_3(-X_K, -Z_{j-2}) & j &= Kf \end{aligned} \quad (38)$$

where

$$S_n(-X_K, Z_j) = K_n(-X_K, Z_j) - K_n(X_{K0}, -Z_j) \quad (39)$$



The final form of the deformation equation is

$$\bar{D}_{K,m} = - C_5 \sum_{j=1,2}^{KO} R(-X_K, -Z_j) P_{j,m} \quad (40)$$

where

$$C_5 = \frac{16P_{HZ}^2}{H_o \pi} \quad (41)$$

#### 2.6.4 Elastohydrodynamic Equation in the Middle Region

(a) The case for pure rolling

The governing equation written at Kth grid point and time

$T_m$  is

$$\begin{aligned} \left( \frac{\partial P}{\partial X} \right)_{K,m} (\bar{H}_{K,m})^3 = & \left( \frac{48U}{H_{om}} \right) (\bar{\mu}_{K,m}) \left\{ \left( \bar{H}_{1,K,m} - \frac{\bar{\rho}_o}{\bar{\rho}_{K,m}} \right) \right. \\ & \left. - \left( \frac{1}{\bar{\rho}_{K,m} H_{om}} \right) \int_{-\infty}^{\infty} \left[ \frac{\partial(\bar{\rho} H_o)}{\partial T} + \bar{f} \left( \frac{\partial \bar{\rho}}{\partial X} + \frac{\partial \bar{\rho}}{\partial T} \right) \right]_m dx \right\} \end{aligned} \quad (42)$$

$$\bar{H}_{K,m} = \bar{H}_{1,K,m} + \frac{\bar{f}_{K,m}}{H_{om}} \quad (43)$$

where

$$\bar{H}_{1,K,m} = 1 + \left( \frac{16P_{HZ}^2}{H_{om}} \right) X_K^2 + \bar{D}_{K,m} \quad (44)$$

$$\bar{f}_{K,m} = \left( \frac{16P_{HZ}^2}{\bar{r}} \right) \left[ (x_{3m} - x_K)^2 - c_4^2 \right] \quad |x_{3m} - x_K| \leq c_4 \quad (45)$$

$$\bar{f}_{K,m} = 0 \quad |x_{3m} - x_K| > c_4$$



The integrand in Eq. (42) can be split into two terms - pressure dependent and independent terms.

$$\begin{aligned} \frac{\partial(\bar{\rho}H_o)}{\partial T} + \bar{f}_{K,m} \left( \frac{\partial \bar{\rho}}{\partial X} + \frac{\partial \bar{\rho}}{\partial T} \right)_{K,m} = - \left[ (\bar{\rho}H_o)_{K,m-1} + f_{K,m} \bar{\rho}_{K,m-1} \right] / \Delta T_m \\ + \left[ (\bar{\rho}H_o)_{K,m} + \bar{f}_{K,m} \bar{\rho}_{K,m} \right] / \Delta T_m + \bar{f}_{K,m} \left( \frac{\partial \bar{\rho}}{\partial X} \right)_{K,m} \end{aligned} \quad (46)$$

The first term in the right hand side of Eq. (46) is independent of  $P_{j,m}$  and is defined as  $\gamma_m(-x_K)$ . The next two terms are dependent of  $P_{j,m}$  and defined as  $\eta_m(-x_K)$ . The absence of deformation term in the integral makes it simpler in obtaining the pressure derivative of the integral and removes the convergence difficulty between two successive iterations.

Using the trapezoidal rule, the integral (42) can be written as:

$$\begin{aligned} \int_{-x_K}^{\infty} \left[ \frac{\partial(\bar{\rho}H_o)}{\partial T} + \bar{f} \left( \frac{\partial \bar{\rho}}{\partial X} + \frac{\partial \bar{\rho}}{\partial T} \right) \right]_m dx = \frac{1}{2} \sum_{i=K}^{KO} \left[ \gamma_m(-x_i) + \eta_m(-x_i) \right] \Delta x_i \\ = I_{K,m} \end{aligned} \quad (47)$$

where

$$\Delta x_i = x_{i+1} - x_{i-1} \quad K+1 \leq i \leq KO-1$$

$$= x_{i+1} - x_i \quad i = K, KO$$

Eq. (30) is expressed in the discretized form at  $-x_{K+1/2}$  and  $T_m$ , where the pressure dependent variables are replaced by their



respective functions.

$$\begin{aligned}
 \psi_m \left( P_{K+1/2} \right) &= \left( \frac{P_{K+1,m} - P_{K,m}}{\Delta X_K} \right) \left\{ 1 + C_6 X_{K+1/2}^2 - C_5 \sum_{j=1}^{K_f} R \left( -X_{K+1/2} - Z_j \right) P_{j,m} \right. \\
 &+ C_7 \left[ \left( X_3 - X_{K+1/2} \right)^2 - C_4^2 \right] \left. \right\} - (C_8) \left( \exp(\bar{\alpha} P_{K+1/2,m}) \right) \\
 &\left\{ \left[ 1 + C_6 X_{K+1/2}^2 - C_5 \sum_{j=1}^{K_f} R \left( -X_{K+1/2} - Z_j \right) P_{j,m} - \frac{\bar{\rho}_o}{1 + \frac{B P_{K+1/2,m}}{1 + A_1 P_{K+1/2,m}}} \right] \right. \\
 &\left. - \frac{I_{K+1/2,m}}{H_{o,m} \left( 1 + \frac{B P_{K+1/2,m}}{1 + A_1 P_{K+1/2,m}} \right)} \right\} \quad (48)
 \end{aligned}$$

where

$$C_6 = \frac{16P_{HZ}^2}{H_{om}}, \quad C_7 = \frac{8P_{HZ}^2}{\bar{r}}, \quad \text{and} \quad C_8 = \frac{48U}{H_{om}}.$$

Eq. (48) is one of the system equations written at  $-X_{K+1/2}$  and  $T_m$ .

Similarly, we can obtain the system equations for the case of rolling and sliding.

$$\begin{aligned}
 \psi_m \left( P_{K+1/2} \right) &= \left( \frac{P_{K+1,m} - P_{K,m}}{\Delta X_K} \right) \left\{ 1 + C_6 X_{K+1/2}^2 - C_5 \sum_{j=1}^{K_f} R \left( -X_{K+1/2} - Z_j \right) P_{j,m} \right. \\
 &+ C_7 \left[ \left( X_{3_m} - X_{K+1/2} \right)^2 - C_4^2 \right] \left. \right\}^3 - (C_8) (1 + b_1) \left( \exp(\bar{\alpha} P_{K+1/2,m}) \right) \\
 &\left\{ \left[ 1 + C_6 X_{K+1/2}^2 - C_5 \sum_{j=1}^{K_f} R \left( -X_{K+1/2} - Z_j \right) P_{j,m} - \frac{\bar{\rho}_o}{1 + \frac{B P_{K+1/2,m}}{1 + A_1 P_{K+1/2,m}}} \right] \right. \\
 &\left. \right\} \quad (49)
 \end{aligned}$$



$$- \frac{I_{K+1/2,m}}{H_{o,m} \left( 1 + \frac{B P_{K+1/2,m}}{1 + A_1 P_{K+1/2,m}} \right)} \} \quad (49)$$

cont.

Applying the Newton-Raphson technique to the system equations, we obtain

$$\{\Psi_m(P)\}^{(n)} + \{\Delta P_m\}^{(n+1)} [\Delta \cdot \Psi_m(P)]^{(n)} = 0 \quad (50)$$

where  $\{\}$  and  $[ ]$  represent a column matrix and a  $N \times N$  matrix respectively, and  $\Delta \cdot$  indicates partial derivative is to be taken with respect to  $P_m$ .  $n$  is the level of iteration.

From Eq. (50) one obtains

$$\{\Delta P_m\}^{(n+1)} = - [\Delta \cdot \Psi_m(P)]^{-1(n)} \cdot \{\Psi_m(P)\}^{(n)} \quad (51)$$

The right hand side of Eq. (51) is assumed to be known from the lower level iteration, and  $\{\Delta P_m\}^{(n+1)}$  is defined as

$$\{\Delta P_m\}^{(n+1)} = \{P_m\}^{(n+1)} - \{P_m\}^{(n)} \quad (52)$$

The elements of matrices in Eq. (51) are detailed in Appendix B.

#### 2.6.5 Calculation of Center Film Thickness

From Eq. (30), the integrated  $Q_{Ko,m}$  is obtained:



$$\begin{aligned}
Q_{Ko,m} &= \frac{48U\bar{\alpha}}{H_o^2 m} \left\{ \int_{-\infty}^0 \left[ \frac{1}{\bar{H}^3} \left( H_1 - \frac{\bar{\rho}_o}{\bar{\rho}} \right) - \left( \frac{1}{\bar{\rho} H_o \bar{H}^3} \right) \int_{-x}^0 \left[ \frac{\partial(\bar{\rho} H_o)}{\partial T} \right. \right. \right. \\
&\quad \left. \left. \left. + \bar{f} \left( \frac{\partial \bar{\rho}}{\partial Z} + \frac{\partial \bar{\rho}}{\partial T} \right) \right] dz \right] dx \right\} \\
&= (48U\bar{\alpha}) \left( \frac{1}{H_o m} \right) \left\{ \int_{-\infty}^0 \frac{1}{\bar{H}^3} \left( H_{1m} - \frac{\bar{\rho}_o}{\bar{\rho}_m} \right) dx \right. \\
&\quad \left. - \frac{1}{H_{om}} \int_{-\infty}^0 \left( \frac{I_x}{\bar{\rho} H^3} \right) dx \right\} \tag{53}
\end{aligned}$$

$$\text{Let } \int_{-\infty}^0 \frac{1}{\bar{H}^3} \left( H_1 - \frac{\bar{\rho}_o}{\bar{\rho}} \right) dx = Q_1$$

$$\text{and } \int_{-\infty}^0 \left( \frac{I_x}{\bar{\rho} H^3} \right) dx = Q_2$$

Then Eq. (53) can be written as

$$Q_{Ko,m} H_{om}^3 + (48U\bar{\alpha}) Q_1 H_{om} + (48U\bar{\alpha}) Q_2 = 0 \tag{54}$$

Eq. (54) is the cubic equation of  $H_{om}$ . Since the coefficient in Eq. (54) implicitly depends upon  $H_{om}$  and  $P_m$ , the analytical solution for  $H_{om}$  is impossible to obtain. Rather, using the so-called secant method,  $H_{o,m}$  is calculated numerically.

#### 2.6.6 Outline of Numerical Procedure

It is assumed that the center pressure is constant while the load and center film thickness change as the asperity moves toward



the center of the contact region. Except for the pressure distribution around the asperity, the pressure profile can be approximated to the Hertzian profile of the same center pressure, which is used as a initial estimated value for pressure at the first time step. The calculation starts with the asperity located far away from the inlet of the contact region.

Written below are the procedures of numerical calculation at each time step:

- 1) At the first time step, the solution for the steady state EHD problem is used. This solution can be taken as a true solution for the transient EHD problem because the asperity located far outside of the inlet of the contact region can not influence the pressure distribution inside the contact region. From the second time step on, the initial estimated pressure is obtained by interpolating the previous pressure distribution for new grid spacings.
- 2) Using the initially estimated pressure distribution, the film thickness, density and viscosity of lubricants are calculated. Also the center film thickness is determined using the pressure and film thickness profiles at the previous times but the new asperity location in the calculation is incorporated. Then the system equations for the calculation of pressure correction in the middle region are solved by the Newton-Raphson technique. The inlet pressure is obtained by the linear-interpolation with the factor  $P_{KA,m}^{(n+1)} / P_{KA,m}^{(n)}$  where



$P_{KA,m}$  is obtained from the system equations, and then the film thickness is calculated using the newly obtained pressure.

- 3) If the converged solution for the pressure in the middle region is obtained, the inlet pressure is recalculated by Eq. (35) and at the same time the center film thickness is also determined. At this time the overall pressure distribution is checked for convergence. If it is converged, the load  $W_m$  is determined by Eq. (33). Otherwise, the procedures (2) and (3) are repeated until the converged solution is obtained.

The computer flow diagram and listing are shown in Appendix C.



## CHAPTER 3

### DISCUSSION OF RESULTS

#### 3.1 Introduction

Since the present study is mainly concerned with the variation of level of the separation between two cylinders, the results are presented as series of film thickness profiles with corresponding pressure distributions as the asperity moves toward the center of the contact region. The asperity height is varied from  $1/2 H_s$  to  $2H_s$  and the asperity width is varied from  $a/4$  to  $a/2$ , where  $H_s$  is the steady state, center film thickness and  $a$  is the Hertzian half-width. The conditions used in the present study are:  $U = 5.3 \times 10^{-12}$ ,  $p_o = 10^5$  psi and  $\bar{\alpha} = 0.95$ .

---

#### 3.2 Pressure Profile

The steady state pressure profile and the corresponding film thickness profile in the absence of the asperity is shown in Fig. 2. These profiles are used as a reference to compare with the transient solutions obtained with the asperity under the same conditions. The pressure profiles in Figs. 3 to 11 show the change in pressure caused by the asperity as it moves from far outside of the contact region to the center. In each series, only three pressure profiles are presented, other intermediate profiles calculated at time intervals between the three positions have been omitted.

In general, the film pressure around the asperity tends to increase, and the increase becomes the largest when the asperity enters the con-



tact region. The increase in pressure is very closely related to the squeezing action of the asperity. The magnitude of the squeezing action increases as it approaches the contact region, and reaching a maximum at the inlet of the contact region. It then starts to diminish as the asperity moves further toward the center. It is evident that the greater the squeezing action, the greater the pressure increase. The pressure fluctuation seems to be insufficient to cause any adverse effect on the contact surface. The elastic depression on the base surface of the asperity did not occur, which is in the direct contrast of the results [ 7 ] in which the pocket is formed elastically when two one-dimensional asperities approach each other.

When the asperity approaches the inlet of the contact region, the inlet pressure gradient becomes very steep. The inlet pressure increases from the ambient value to a very high pressure in a short distance. The lubricant behind the asperity is less pressurized while the lubricant in the front of the asperity is severely pressurized by the squeezing action of the asperity.

Shown in Figs. 10 and 11 are the results of the rolling and sliding of the two cylinders. Fig. 10 is the result for  $U_1 = 0.9U$  and  $U_2 = 1.1U$ , and Fig. 11 is the result for  $U_1 = 1.1U$  and  $U_2 = 0.9U$ . Both pressure profiles have the small local pressure peak when the asperity is in the contact region. As mentioned previously, the rolling term and the squeezing term of the asperity do not cancel out each other. Thus, even when the asperity moves in parallel with the flat surface, the squeezing action is still possible allowing positive and negative pressure on the lubricant in either side of the asperity. However, when the asperity is near the inlet of



the contact region, the squeezing action overcomes the sliding term and consequently the pressure bump is not generated in the fluid film. When the asperity moves faster than the lower cylinder, the pressure in the left side of the asperity changes more rapidly, and the reduction in pressure is quite substantial compared with the pressure profile with the asperity entering the inlet of the contact region.

### 3.3 Film Thickness

The steady state film thickness profile in the contact region is approximately parallel with the flat surface, and the thickness is dependent upon a rolling speed if other conditions are the same. Since the conditions in both steady and transient problems are the same, the quantitative comparison between them can be made with regard to the effect of an asperity.

~~The shape of the transient film thickness profile is notably different from the steady state profile. The steady state case profile is approximately constant across the contact width, whereas the transient film profile is sloped considerably toward the contact center. The slope of the film thickness profile increases with increasing asperity height. This phenomena helps in preventing the direct contact of the asperity tip and the flat surface. As far as the shape of the film thickness profile is concerned, the influence of width of the asperity is not significant even though the wider asperity tends to increase the level of the contact separation significantly.~~

In all cases studied, the center film thickness is always larger than that for the steady state case. The increase in center film thickness is dependent upon the asperity height, and the level of separation



increases with increasing height of the asperity. Even for the asperity with the height equal to twice that of the steady state film thickness  $H_s$ , the tip of the asperity does not touch the flat surface when it passes through the first half of the contact region. This means that the level of separation increases more than 100% of  $H_s$ . This result may be one of the most significant findings in the present study and appears to lend credence to previous speculations regarding the beneficial effect of the asperity on the film thickness.

Displayed in Fig. 12 is the center film thickness vs. the asperity location curves, which shows that the center film thickness increases continuously as the asperity moves toward the contact center. The rate of increase in the center film thickness is dependent upon the width and height of the asperity. For the same height of the asperity, the center film thickness for a wider asperity increases faster and larger than that for a narrower asperity. When there is sliding between the two cylinders, the change in center film thickness depends upon a speed of the cylinder to which the asperity is attached. In the present study the asperity is attached to the upper cylinder. The results show that if the upper cylinder moves faster than the lower cylinder with the same rolling speed of pure rolling, the center film thickness increases more than the one for the case of pure rolling having the same asperity geometry. In the opposite case, that is, when the lower cylinder moves faster than the upper cylinder, the increase in center film thickness is less than that for the case of pure rolling. The faster the upper cylinder can pressurize the lubricant more effectively in the contact region. Consequently, the level of separation tends to increase to accommodate the lubricant swept in by the asperity.



Fig. 13 shows the relationship between the inlet minimum film thickness and the asperity height, both of which are normalized by the steady state film thickness to show the extent of the increase of the center film thickness by the asperity. The dash line in Fig. 13 indicates the relation between these two values if the center film thickness is not raised by the hydrodynamic effect of the asperity. For small asperity heights ( $f/h_s \ll 1$ ), the solid lines coincide with the dash line indicating an absence of hydrodynamic effect due to the asperity. For large asperity heights ( $f/h_s > 1$ ) the dash line indicates a negative minimum film or an interference, whereas the solid lines still show a clearance between the tip of asperity and the opposing surface. Even for the very severe case of  $f/h_s = 2$ , a clearance of approximately 10-20% of the steady state film thickness was found to exist underneath the tip of the asperity.

---

### 3.4 Load

It was found that the load carrying capacity of two cylinders with an asperity is larger than that for two cylinders without an asperity. However, the increase is not more than 15% of the steady state load with the same peak pressure. Furthermore, in the load calculation the pressure distribution in the second half of the contact region is assumed to be a Hertzian pressure profile. Thus, it may be possible that the load may change unfavorably when the asperity enters the second half of the contact region, which remains to be investigated.



## CHAPTER 4

### SUMMARY OF RESULTS

The important aspects of elastohydrodynamic lubrication, with a single, one-dimensional asperity, have been found by solving numerically the coupled transient Reynolds equation and the elasticity equation. Even though the assumption of a single asperity is highly ideal, but this study sheds some light on the effect of surface roughness on elastohydrodynamic lubrication.

The results show that:

- 1) The film pressure tends to increase more than the steady state pressure, and in particular, the increase in pressure reaches a maximum as the asperity approaches the inlet of the contact region. The asperity height and the pressure increase above the steady state pressure are closely related to each other; the higher the asperity height, the larger the pressure increase. In the pure rolling case, it has been found that a local pressure peak is not developed. However, in the cases of sliding and rolling, a small, local pressure peak is developed on the pressure profile when the asperity moves into the contact region.
- 2) In general, the overall film thickness profile increases with increasing asperity height, but is not significantly affected by the asperity width. Moreover, the slope of the overall film thickness profile for the transient cases is much greater than the steady state profile which is approximately constant across the contact width. The increase in the center



film thickness also depends upon the width and height of the asperity. Even for the case of an asperity height of  $2H_s$ , the center film thickness increases more than 100% compared to the steady state center film thickness.

As mentioned before, the surface condition employed in the present study is highly ideal. Thus, the present results may not be applicable to a more realistic surface condition of randomly distributed asperities. However, the results of the present study suggest that the rough contact surface is beneficial in generating continuous fluid film between the heavily loaded, two contact surfaces.



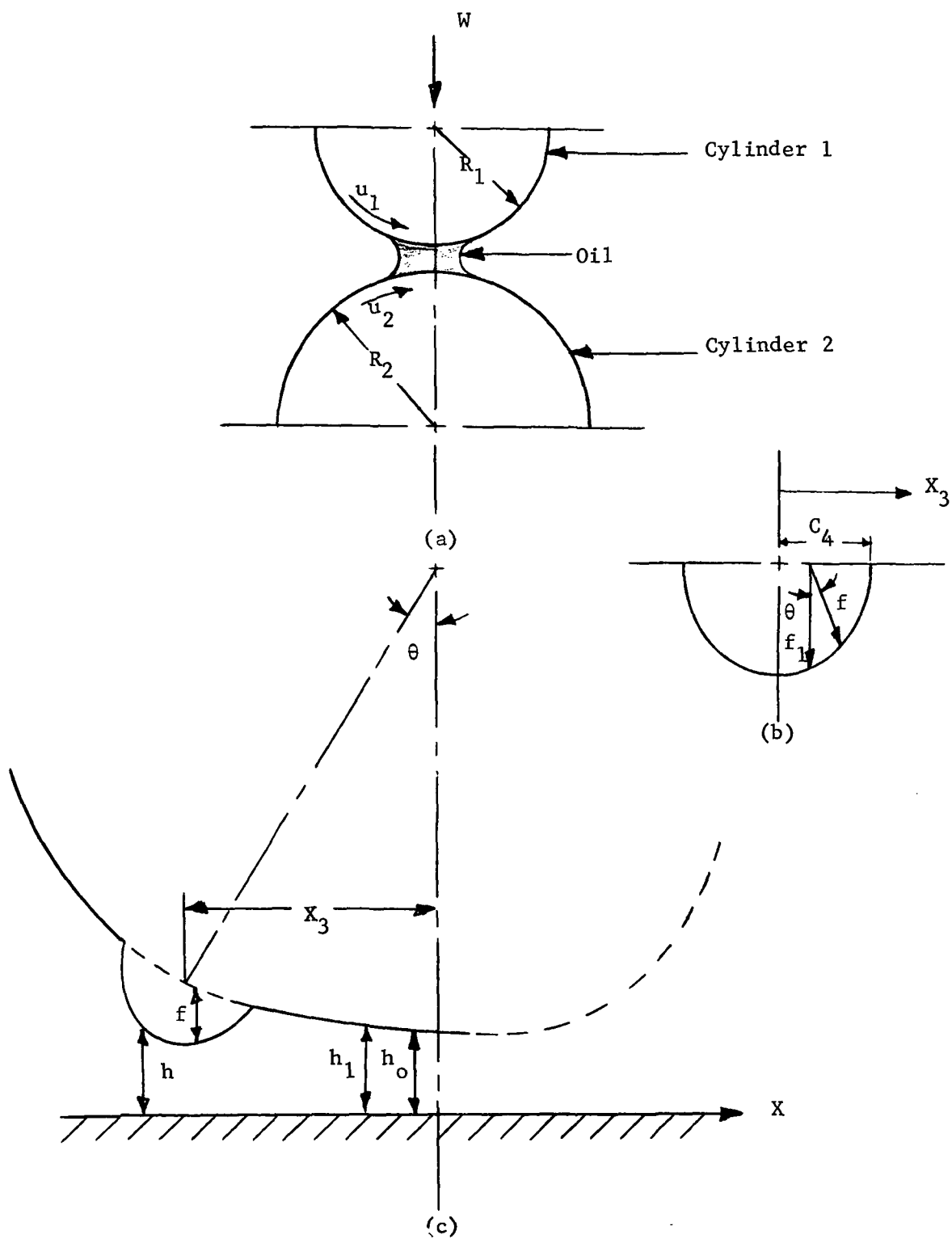


Fig. 1 Geometry of the elastohydrodynamic problem with an asperity.



Straight Exponential Lubricant Model  
 $G = 3180$   
 Center Pressure,  $P_0 = 1.0 \times 10^5$  psi

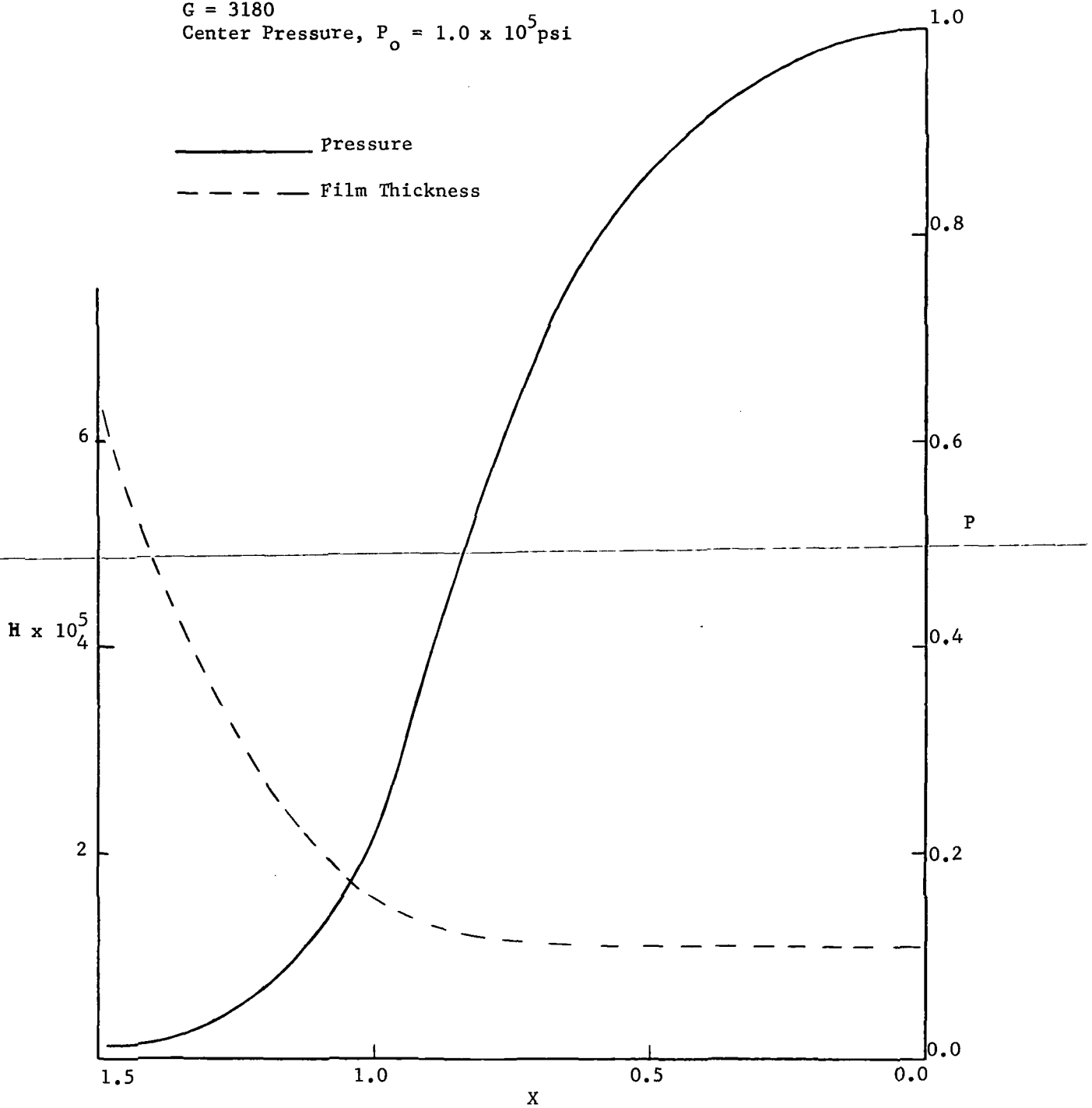


Fig. 2 Pressure and film thickness profiles without an asperity, pure rolling.



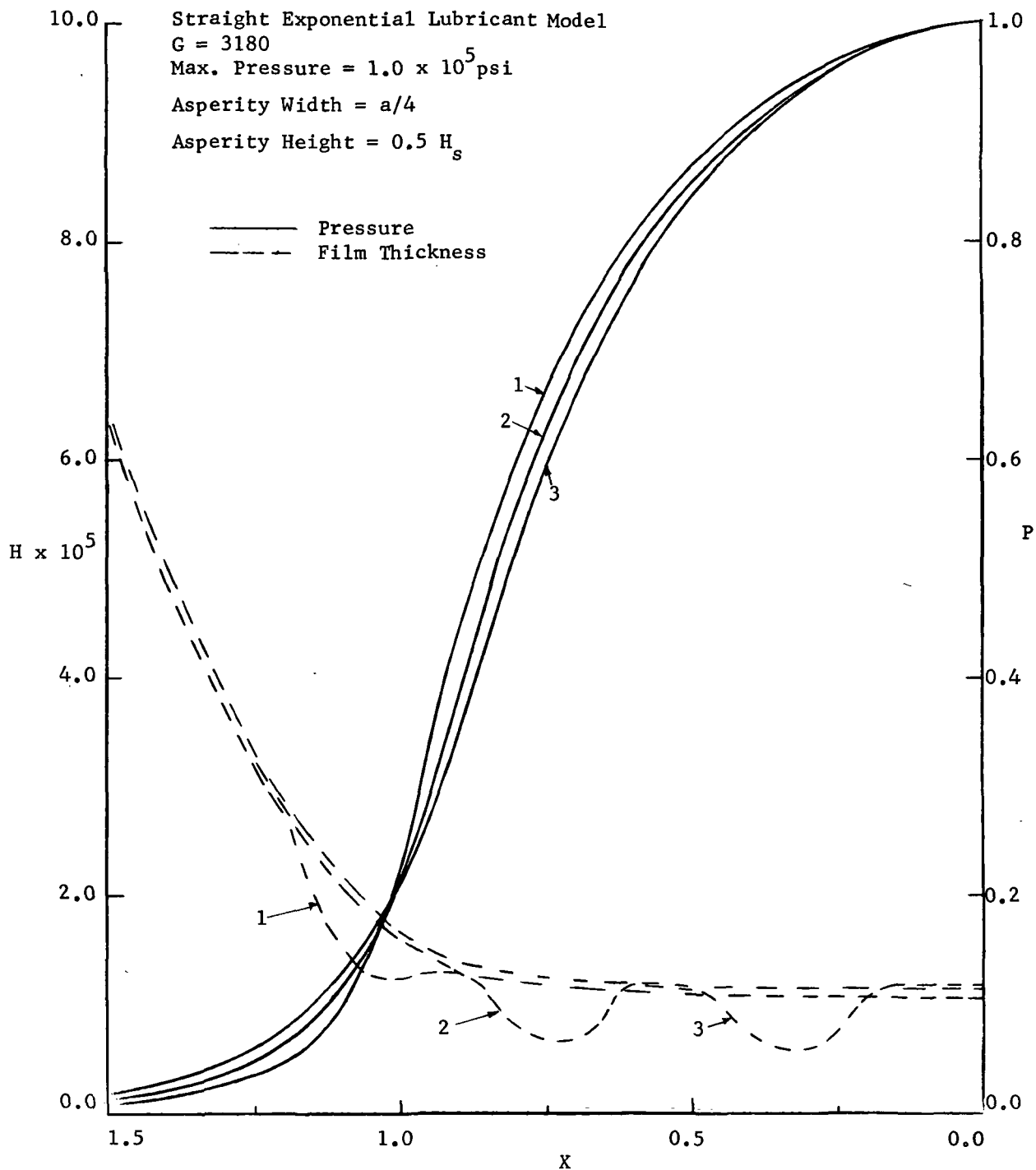


Fig. 3 Pressure and film thickness profiles with an asperity, pure rolling, asperity width =  $a/4$  and Height =  $H_s/2$ .



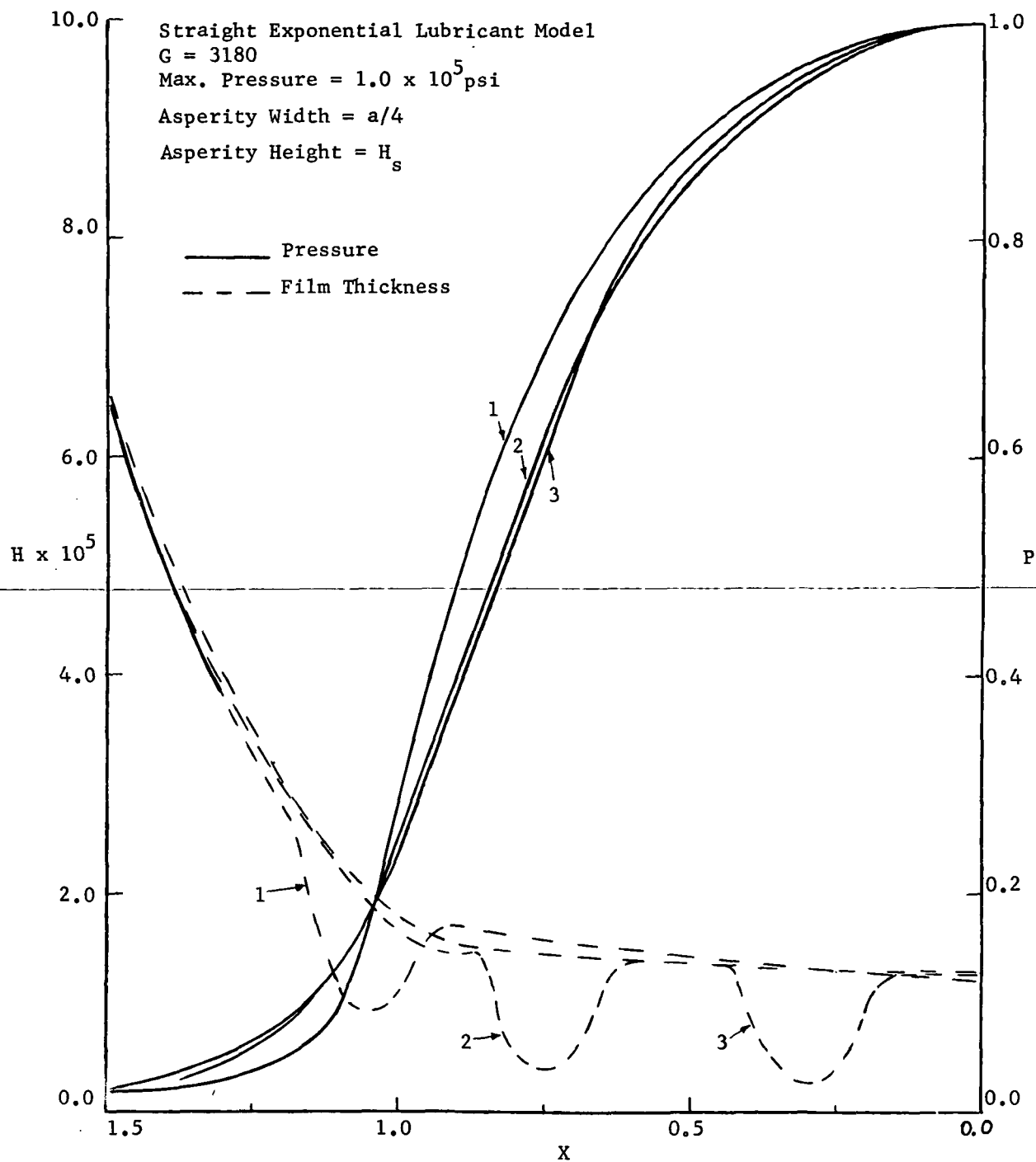


Fig. 4 Pressure and film thickness profiles with an asperity, pure rolling, asperity width =  $a/4$  and height =  $H_s$ .



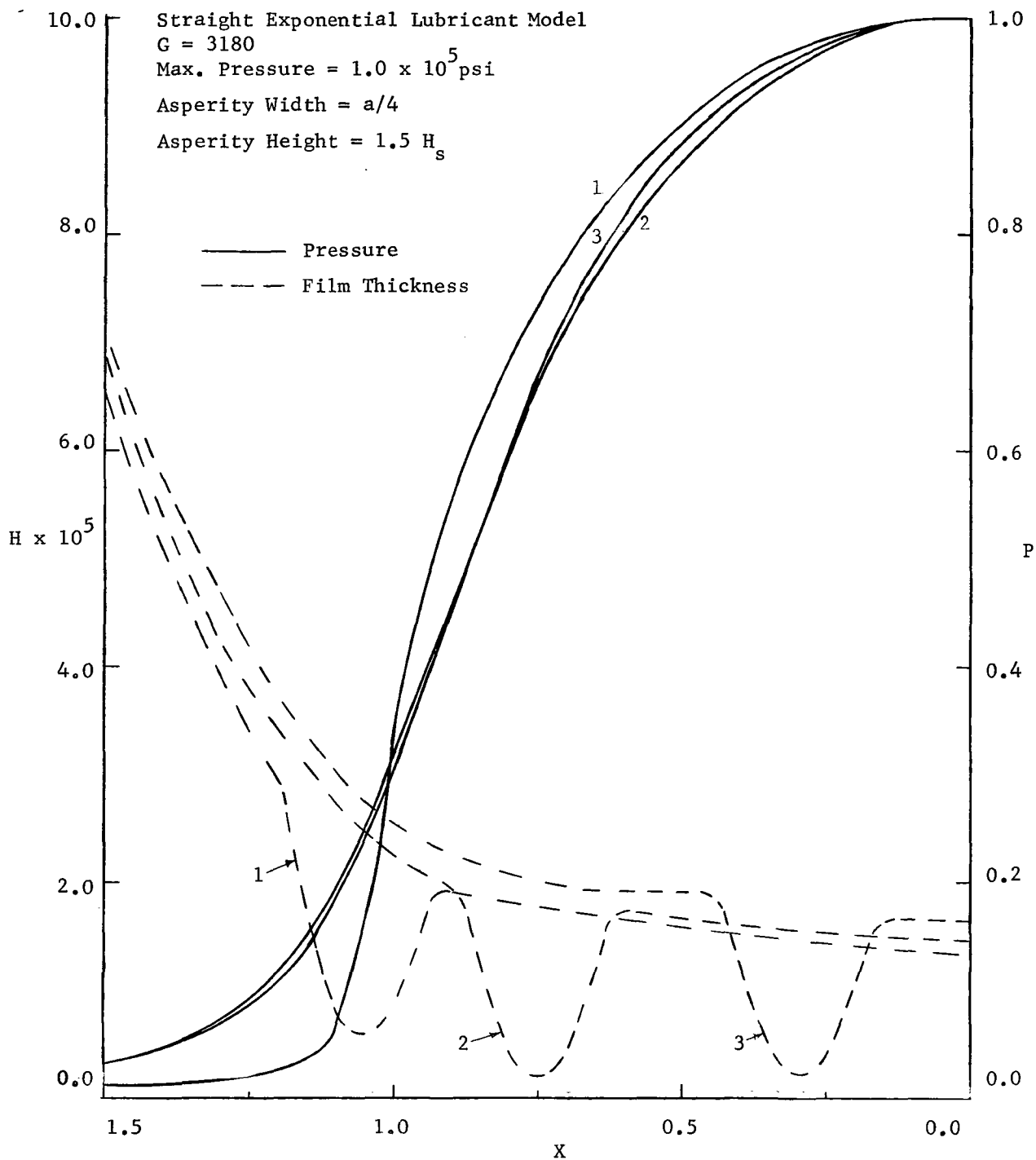


Fig. 5 Pressure and film thickness profiles with an asperity, pure rolling, asperity width =  $a/4$  and height =  $1.5 H_s$ .



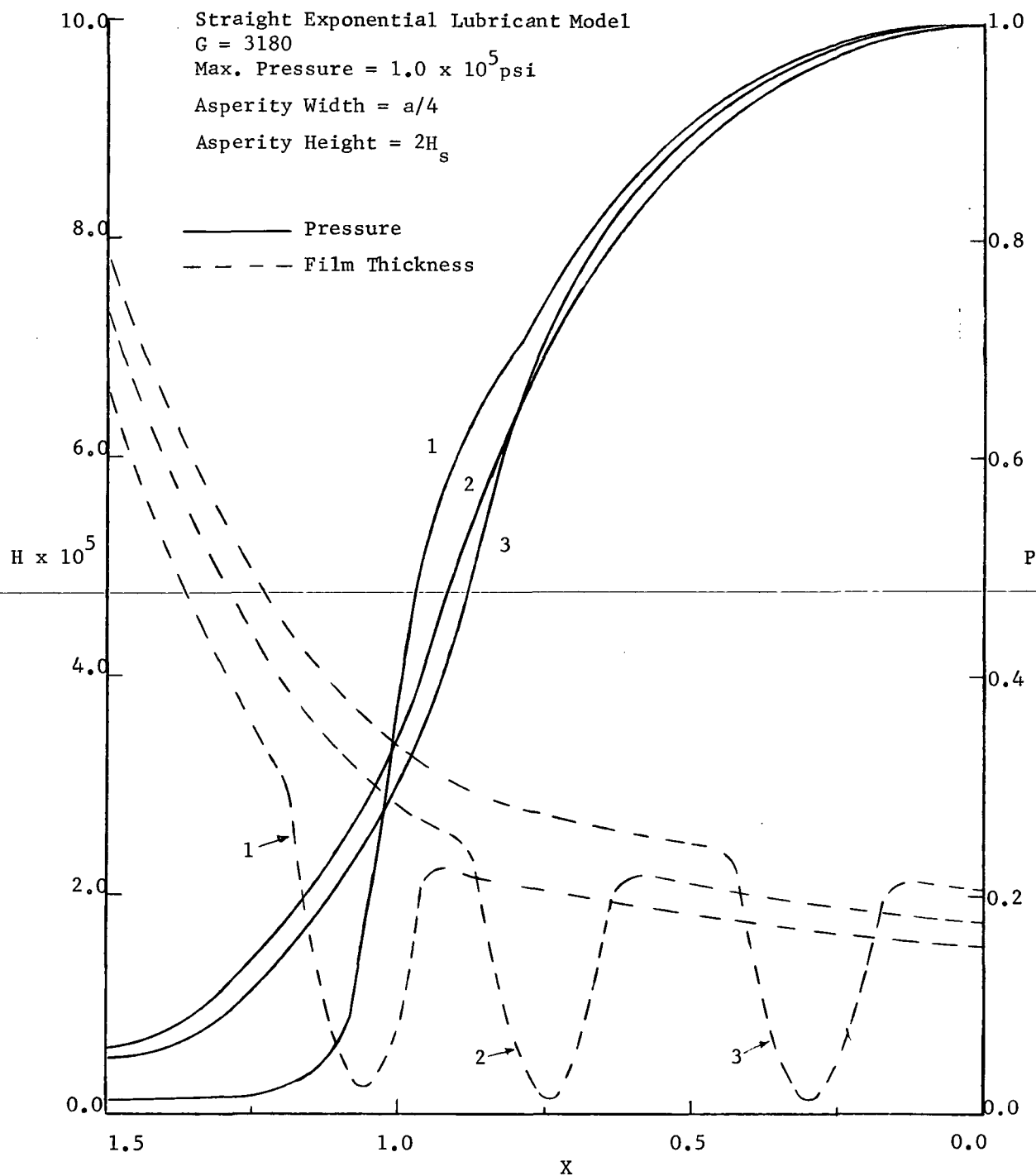


Fig. 6 Pressure and film thickness profiles with an asperity, pure rolling, asperity width =  $a/4$  and height =  $2H_s$ .



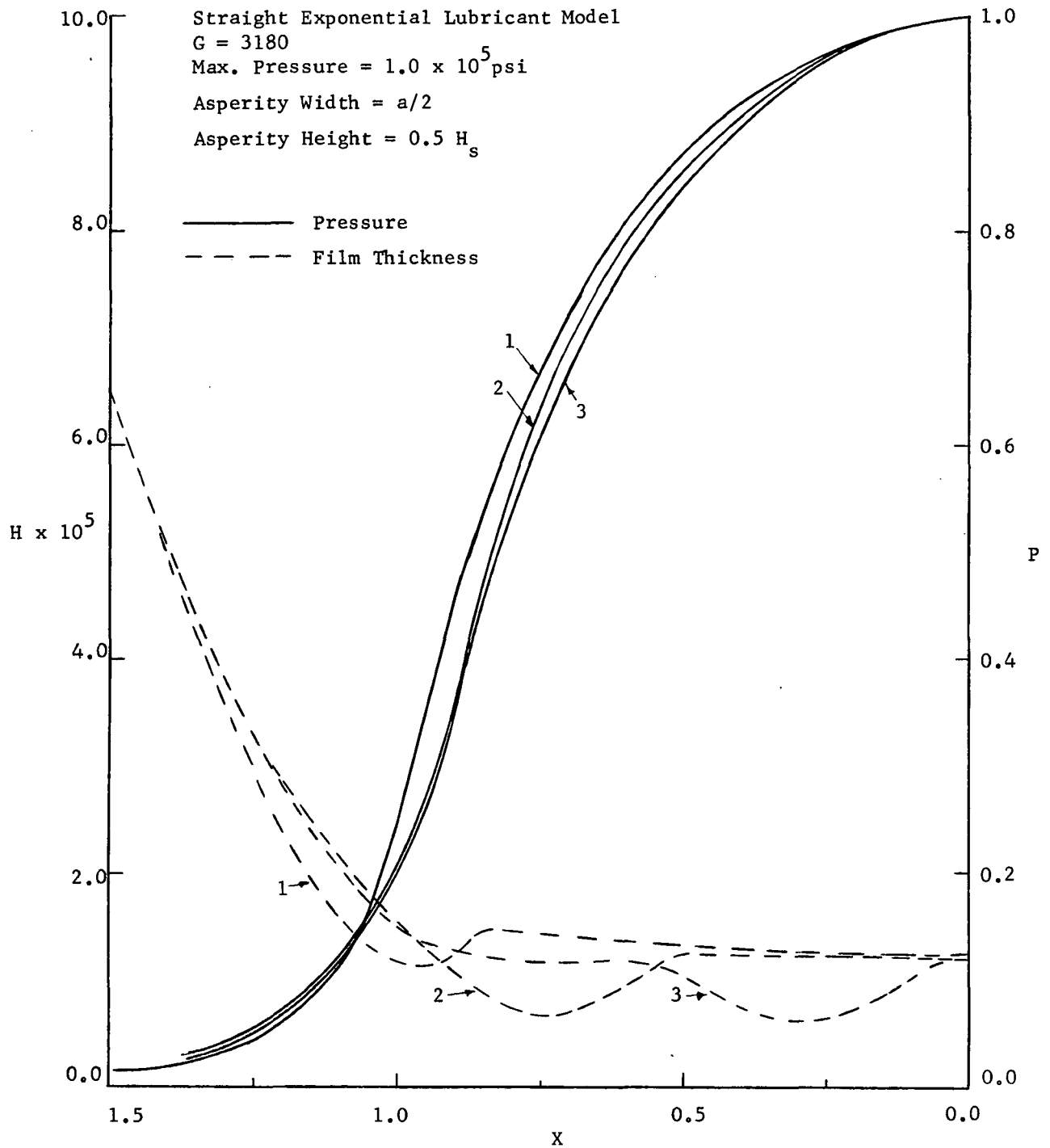


Fig. 7 Pressure and film thickness profiles with an asperity, pure rolling, asperity width =  $a/2$  and height =  $H_s/2$ .



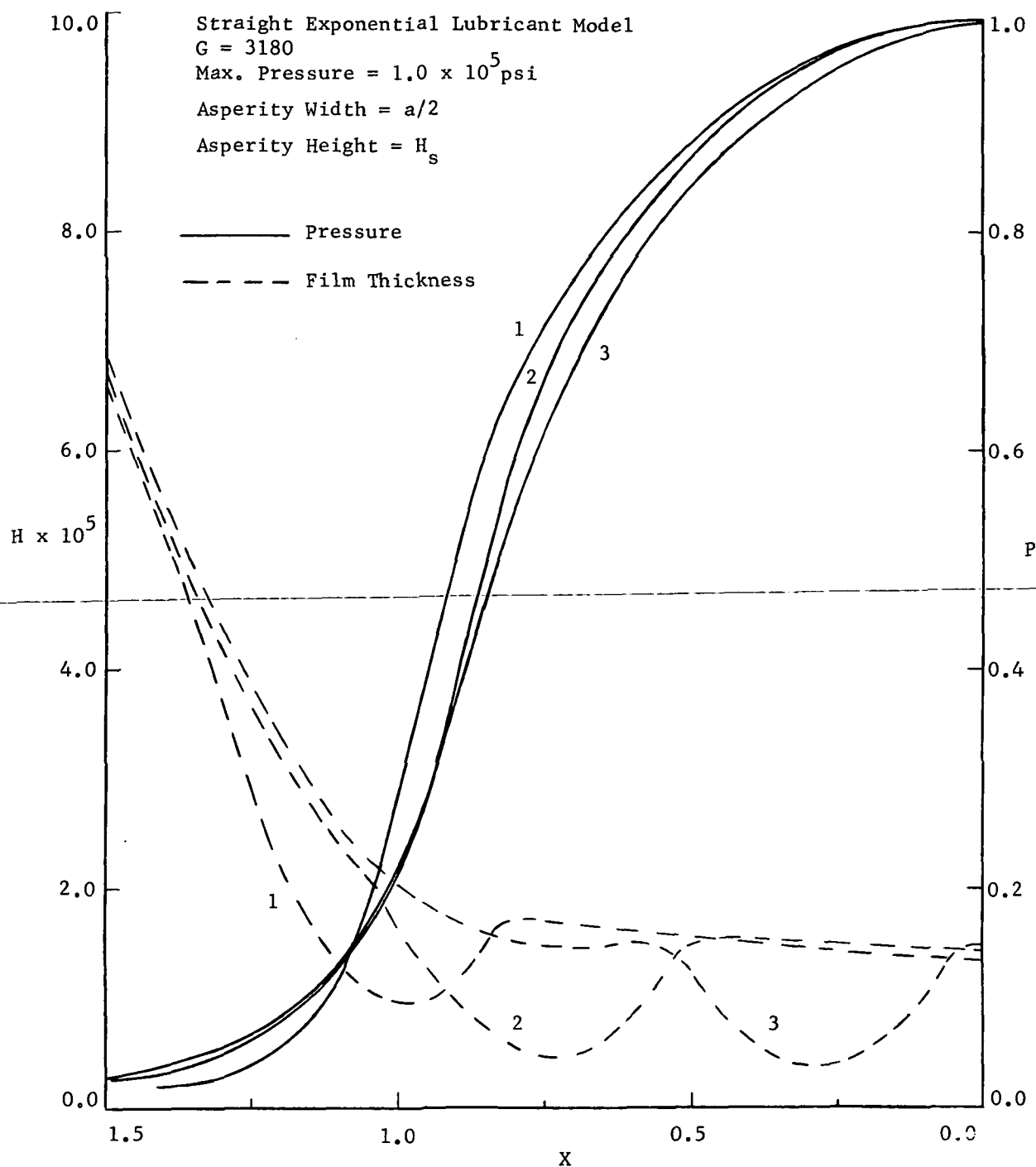


Fig. 8 Pressure and film thickness profiles with an asperity, pure rolling, asperity width =  $a/2$  and height =  $H_s$ .



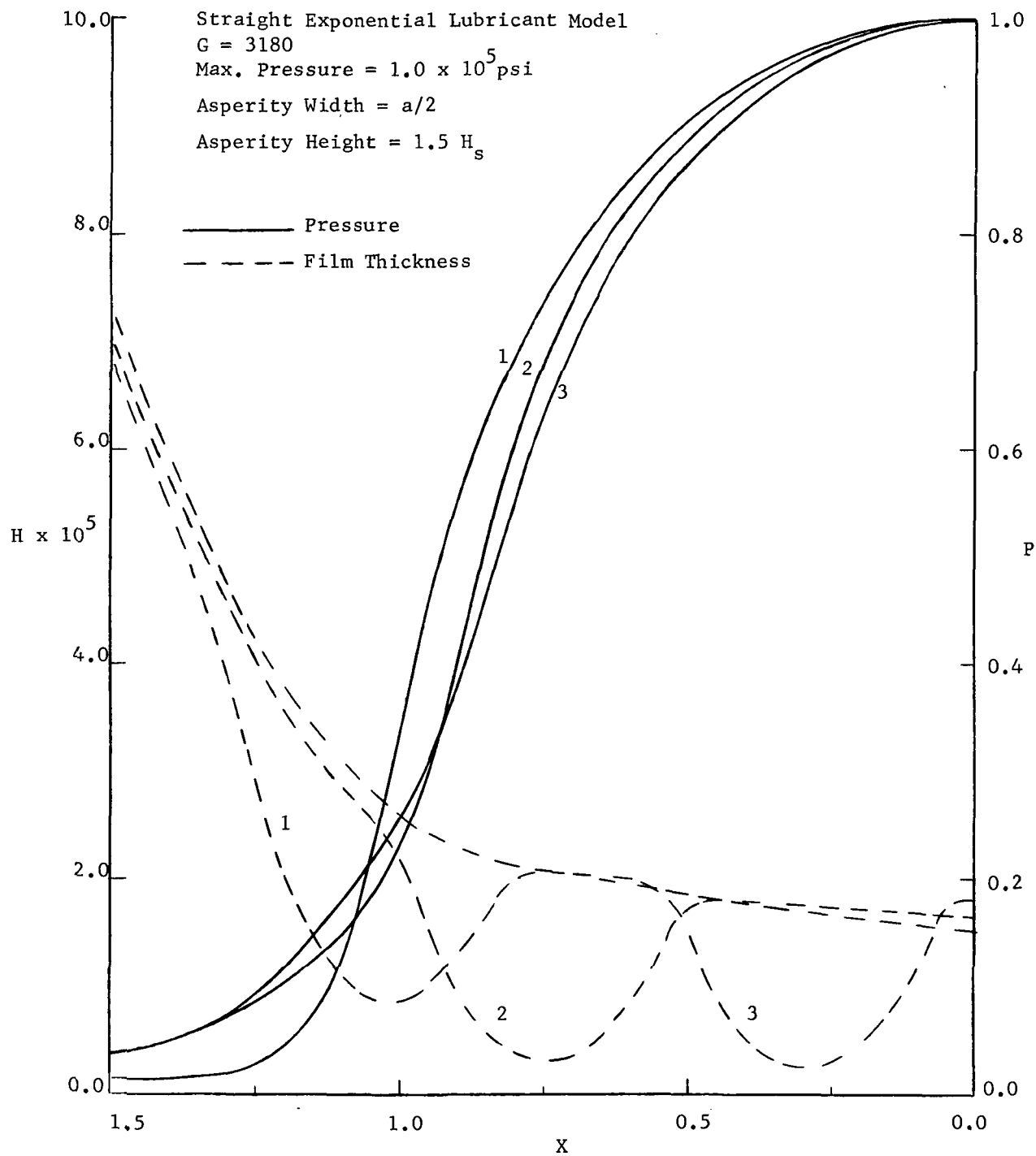


Fig. 9 Pressure and film thickness profiles with an asperity, pure rolling, asperity width =  $a/2$  and height =  $1.5 H_s$ .



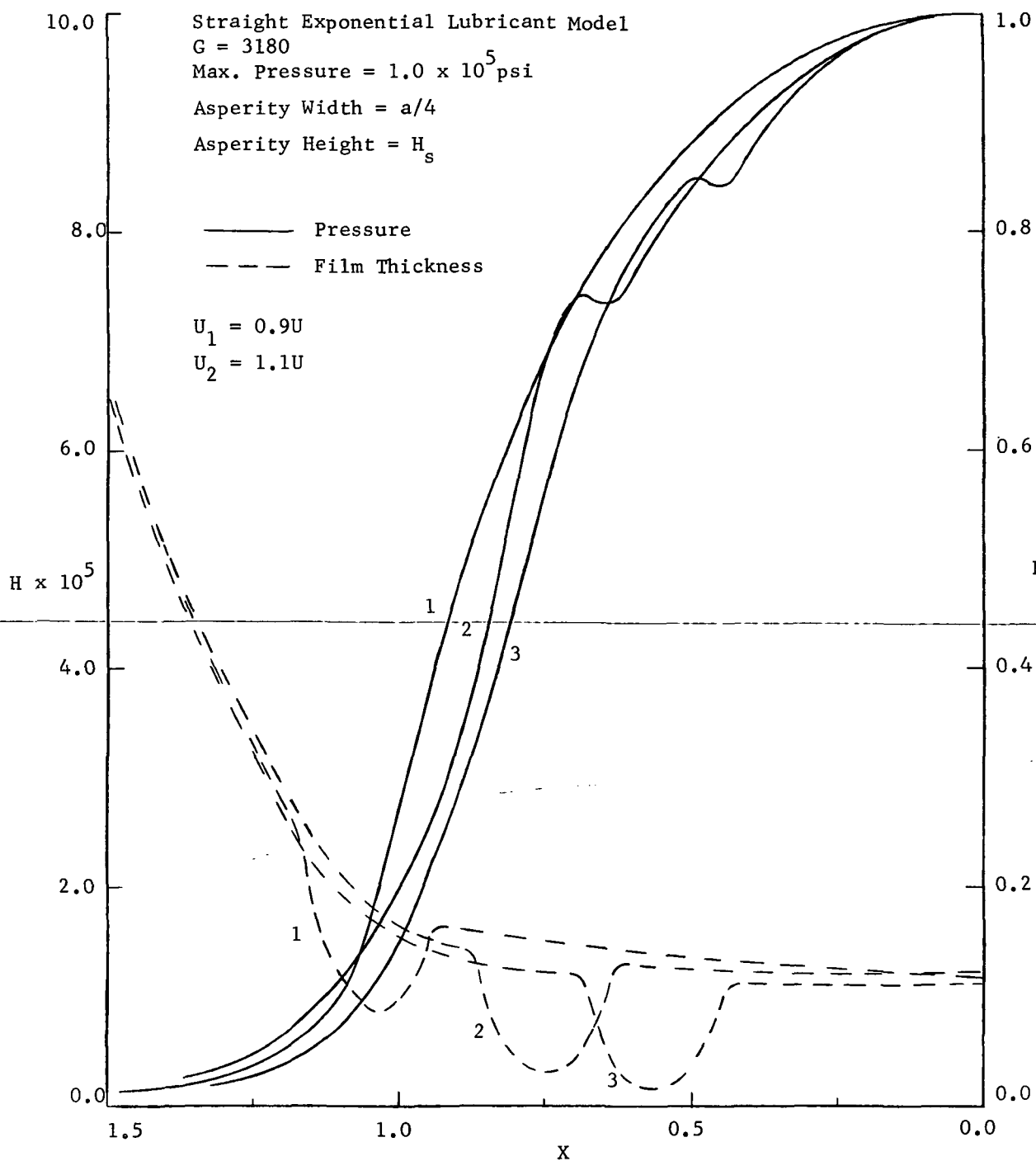


Fig. 10 Pressure and film thickness profiles with an asperity, rolling and sliding, asperity width =  $a/4$  and height =  $H_s$ ,  $U_1 = 0.9U$ ,  $U_2 = 1.1U$ .



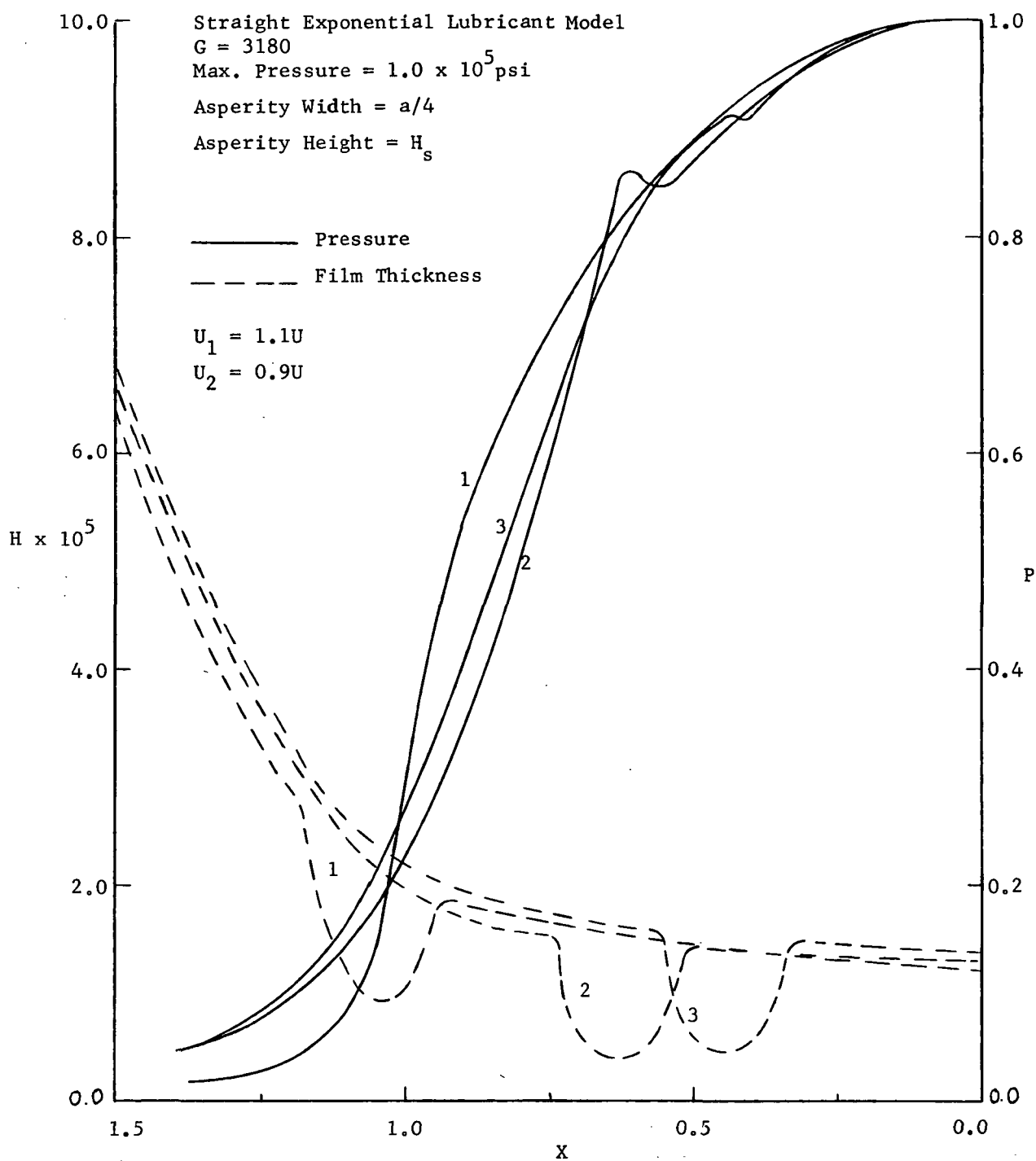


Fig. 11 Pressure and film thickness profiles with an asperity, rolling and sliding asperity width =  $a/4$  and height =  $H_s$ ,  $U_1 = 1.1U$ ,  $U_2 = 0.9U$ .



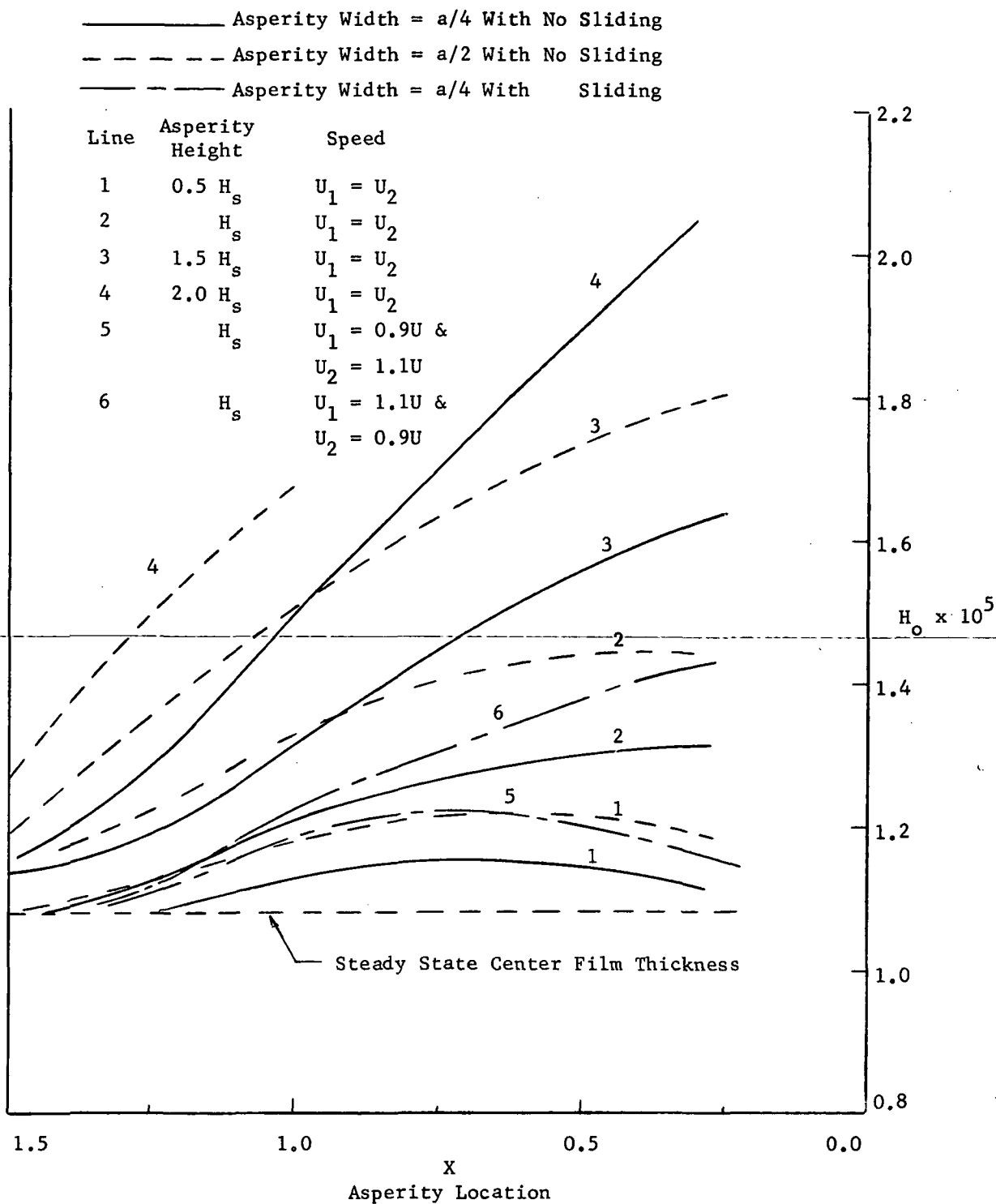


Fig. 12 Center film thickness vs. asperity locations.



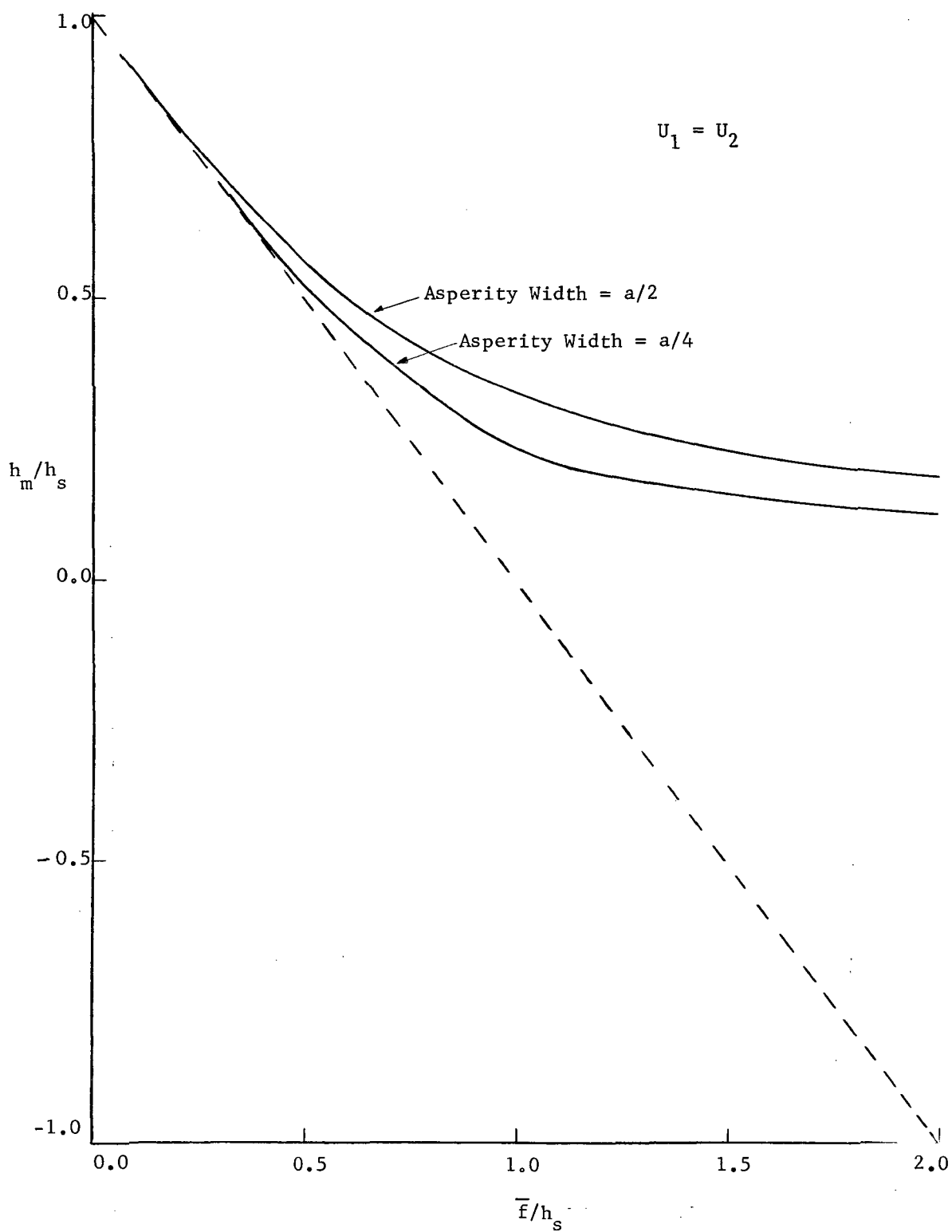


Fig. 13 Minimum film thickness ratio ( $h_m/h_s$ ) vs. asperity height ratio ( $\bar{f}/h_s$ ).



APPENDIX A  
SYMBOLS LIST

a	Half of Hertzian width
$a_1$	coefficient of density
$A_1 = \frac{a}{P_o}$	
b	coefficient of density
$B = \frac{b}{P_o}$	
c	constant in deformation formula
$c_1$	constant in deformation formula of cylinder 1
$c_2$	constant in deformation formula of cylinder 2
$c_3$	coefficient of deformation formula
$c_4$	half width of asperity
$C_4 = \frac{c_4}{a}$	
d	Deformation
$\overline{D} = \frac{d}{h_o}$	
$D = \frac{d}{R}$	
$E = 2 \left[ \frac{1-\nu_1^2}{E_1} + \frac{1-\nu_2^2}{E_2} \right]^{-1}$	Equivalent Young' modulus
$E_1$	Young's modulus of cylinder 1
$E_2$	Young's modulus of cylinder 2
f	Height of Asperity
$\overline{f} = \frac{f}{R}$	
$G = \alpha E$	
h	Film thickness
$h_1$	See Eq. (7)



$$\bar{H} = \frac{h}{h_o}$$

$$H = \frac{h}{R}$$

$$H_1 = \frac{h_1}{h_o}$$

$$h'_o$$

Rigid center film thickness

$$h_o$$

center film thickness

$$H_o = \frac{h_o}{R}$$

$$h_g$$

geometrical film thickness

$$H_g = \frac{h_g}{R}$$

$$h_m$$

Minimum film thickness

$$H_m = \frac{h_m}{R}$$

$$H_s = \frac{h_s}{R}$$

$$i$$

A dummy index

$$I_{K,m}$$

See Eq. (B.7)

$$j$$

A dummy index

$$k$$

A dummy index

$$m$$

A index for time step

$$P$$

Pressure

$$P_o$$

Center pressure

$$P = \frac{P}{P_o}$$

$$P_{HZ} = \frac{P_o}{E}$$

Hertzian pressure

$$Q = 1 - \frac{1}{\mu}$$



$r$	See Fig. 1
$\bar{r} = \frac{r}{R}$	
$R = \frac{R_1 \times R_2}{R_1 + R_2}$	Radius of equivalent cylinder
$R_1$	Radius of cylinder 1
$R_2$	Radius of cylinder 2
$RR_{K,j}$	See Eq. (A.10)
$t$	time
$T = \frac{u_1}{R}t$	For Part II
$s_j = \frac{u_j^2}{2}(\ell_n  u_j  - \frac{3}{2})$	
$u_j = -Z_j - X_K$	
$u_1$	Speed of upper cylinder
$u_2$	Speed of lower cylinder
$U = \frac{\mu_s u_1}{ER}$	



$x$	coordinate along film
$x_3$	Instantaneous location of asperity
$X = \frac{x}{a}$	
$X_3 = \frac{x_3}{a}$	
$X_{KA}$	Coordinate separating the inlet and middle region
$X_{KA} = \frac{X_{KA}}{a}$	
$w$	Load per unit width of cylinder
$W = \frac{w}{ER}$	
$\xi$	Dummy coordinate along film
$Z = \frac{\xi}{a}$	
$\nu_1$	Poisson's ratio of cylinder 1
$\nu_2$	Poisson's ratio of cylinder 2
$\rho$	Density
$\rho_s$	Ambient density
$\bar{\rho} = \frac{\rho}{\rho_s}$	
$\mu$	viscosity
$\mu_s$	Ambient viscosity
$\bar{\mu} = \frac{\mu}{\mu_s}$	



$\alpha$  Pressure-viscosity coefficient  
 $\bar{\alpha} = \alpha P_o$

$\beta$  Second pressure-viscosity coefficient  
 $\bar{\beta} = \beta$

$\Psi_m(p)$  System equation

$\Delta \cdot \Psi_m(p)$  Derivative of  $\Psi_m(p)$  with respect to  $p_m$

$D = \frac{d}{R}$

$\bar{H} = \frac{h}{h_o}$



## APPENDIX B

### CALCULATION OF MATRIX ELEMENTS IN EQ. (50)

$[\Delta \cdot \Psi_m(P)]$  in Eq. (50) has  $N \times N$  elements, each one of which is the derivative of  $\Psi_m(P)$  with respect to  $P_m$ . For convenience,  $\Psi_m(P)$  is written below,

$$\begin{aligned} \Psi_m(P_{K+1/2}) = & \left( \frac{P_{K+1,m} - P_{K,m}}{\Delta X_K} \right) \left\{ 1 + C_6 X_{K+1/2}^2 - C_5 \sum_{j=1}^{K_f} R(-X_{K+1/2}, -Z_j) P_{j,m} \right. \\ & + C_7 \left[ (X_3 - X_{K+1/2})^2 - C_4^2 \right]^3 - (C_8) \left( \exp(\bar{\alpha} P_{K+1/2,m}) \right) \\ & \left. \left\{ \left[ 1 + C_6 X_{K+1/2}^2 - C_5 \sum_{j=1}^{K_f} R(-X_{K+1/2}, -Z_j) P_{j,m} \right. \right. \right. \\ & \left. \left. - \frac{\bar{\rho}_o}{1 + \frac{B P_{K+1/2,m}}{1 + A_1 P_{K+1/2,m}}} \right] - \frac{I_{K+1/2,m}}{H_{om} \left( 1 + \frac{B P_{K+1/2,m}}{1 + A_1 P_{K+1/2,m}} \right)} \right\} \end{aligned} \quad (48)$$

Eq. (48) is EHD equation in which viscosity, density and film thickness are expressed as a function of pressure. Before differentiation, the algebraic average of these variables is identified at  $-X_{K+1/2}$ , and Eq. (48) is expressed in the following form:

$$\begin{aligned} \Psi_m(P_{K+1/2}) = & \left( \frac{P_{K+1,m} - P_{K,m}}{\Delta X_K} \right) \left( \frac{1}{2} \right) \left( \bar{H}_{K+1,m} + \bar{H}_{K,m} \right)^3 - (C_8) \left( \bar{\mu}_{K+1/2,m} \right) \\ & \left\{ \left[ \left( \frac{1}{2} \right) \left( \bar{H}_{K+1,m} + \bar{H}_{K,m} \right) - \frac{\bar{\rho}_o}{\bar{\rho}_{K+1/2,m}} \right] \right\} \end{aligned} \quad (A-1)$$



$$- \left(\frac{1}{2}\right) \left( \frac{1}{H_{om} \bar{\rho}_{K+1/2,m}} \right) (I_{K+1,m} + I_{K,m}) \} \quad (A-1) \text{ cont.}$$

where

$$I_{K,m} = \left(\frac{1}{2}\right) \sum_{i=K}^{KO} [\gamma_m(-x_i) + \eta_m(-x_i)] \Delta x_i$$

and the film thickness  $H_{K+1/2,m}$  and the integral  $I_{K+1/2,m}$  are expressed as the average of the two values at  $-x_K$  and  $-x_{K+1/2}$  as:

$$I_{K+1/2,m} = \frac{1}{2} (I_{K+1,m} + I_{K,m}) \quad (A-2)$$

$$\bar{H}_{K+1/2,m} = \frac{1}{2} (\bar{H}_{K+1,m} + \bar{H}_{K,m}) \quad (A-3)$$

$$\bar{H}_{1K+1/2,m} = \frac{1}{2} (\bar{H}_{1K+1,m} + \bar{H}_{1K,m}) \quad (A-4)$$

$\bar{H}_{K+1/2,m}$  is the film thickness including the height of the asperity and

$\bar{H}_{1K+1/2,m}$  is the film thickness excluding the height of the asperity.

$\bar{\rho}_{K+1/2,m}$  and  $\bar{\mu}_{K+1/2,m}$  are assumed to be a function of the average pressure,  $\frac{1}{2} (P_{K+1,m} + P_{K,m})$  as:

$$\bar{\rho}_{K+1/2,m} = \frac{\frac{1}{2} B (P_{K+1,m} + P_{K,m})}{1 + \frac{1}{2} A_1 (P_{K+1,m} + P_{K,m})} \quad (A-5)$$

$$\bar{\mu}_{K+1/2,m} = \exp \left[ \frac{1}{2} \bar{\alpha} (P_{K+1,m} + P_{K,m}) \right] \quad (A-6)$$

Eqs. (D-2) to (D-6) are differentiated with respect to  $P_{j,m}$ , where

$\bar{H}_{K+1/2,m}$  and  $\bar{H}_{1K+1,m}$  are the functions of  $P_{j,m}$  regardless of indice  $j$



and the rest of Eqs. (D-2), (D-5) and (D-6) are the function of  $P_{j,m}$  only for  $j = K$  or  $K+1$ . The derivatives of these equations are written as:

$$\frac{\partial H_{K+1/2,m}^3}{\partial P_j} = - (3C_5 RR_{K,j}) (\bar{H}_{K+1,m} + \bar{H}_{K,m})^2 \quad (A-7)$$

where

$$RR_{K,j} = R(-X_{K+1}, -Z_j) + R(-X_K, -Z_j) \quad \text{for } j = KA, KA+1$$

$$RR_{K,j} = \sum_{i=1}^{KA} \left\{ \left[ R(-X_{K+1}, -Z_i) + R(-X_K, -Z_j) \right] \left( \frac{P_{i,m}}{P_{KA,m}} \right) \right\} \quad \text{for } j = KA, KA+1$$

To account for the effect of inlet pressure distribution on  $D_{KA,m} + D_{KA+1,m}$ , the sum of the product of the deformation kernel and inlet pressure ratio is considered as the derivative of the deformations at  $-X_{KA}$  and  $-X_{KA+1}$  with respect to  $P_{KA,m}$  and  $P_{KA+1,m}$ .

For  $j = K, K+1$ ,

$$\frac{\partial \bar{\mu}_{K+1/2,m}}{\partial P_{j,m}} = \frac{1}{2} \bar{\alpha} \bar{\mu}_{K+1/2,m} \quad (A-8)$$

$$\frac{\partial \bar{\rho}_{K+1/2,m}}{\partial P_{j,m}} = \frac{B}{2 + A_1 (P_{K+1,m} + P_{K,m})} \quad (A-9)$$

$$\frac{\partial I_{K,m}}{\partial P_{j,m}} = \left( \frac{1}{2} \right) \left( \frac{H_{om} + \bar{f}_{K,m}}{\Delta T_m} + \frac{\bar{f}_{K,m}}{\Delta X_K} \right) \left( \frac{\partial \bar{\rho}_K}{\partial P_{j,m}} \right) (\Delta X_K) \quad (A-10)$$

For  $j \neq K, K+1$ , Eqs. (D-8), (D-9) and (D-10) is zero.



Using Eqs. (D-7), (D-8), (D-9) and (D-10), the derivative of

$\Psi_m(P_{K+1/2})$  is written as:

$$\begin{aligned}
\frac{\partial \Psi_m(P_{K+1/2})}{\partial P_{j,m}} &= \left( \frac{P_{K+1,m} - P_{K,m}}{\Delta X_K} \right) (-1.5 C_5 RR_{K,j}) (\bar{H}_{K+1,m} + \bar{H}_{K,m})^2 \\
&+ (\delta_g) \left( \frac{1}{2} \right) (\bar{H}_{K+1,m} + \bar{H}_{K,m})^3 \left( \frac{1}{\Delta X_K} \right) - (C_8) (\bar{\alpha} \exp(\bar{\alpha} P_{K+1/2,m})) \\
&\left\{ \left[ \frac{1}{2} (\bar{H}_{K+1,m} + \bar{H}_{K,m}) - \frac{\bar{\rho}_o}{\bar{\rho}_{K+1/2,m}} \right] - \frac{1}{2} \left( \frac{1}{H_{om} \bar{\rho}_{K+1/2,m}} \right) (I_{K+1,m} + I_{K,m}) \right\} \\
&- (C_8) (\exp(\bar{\alpha} P_{K+1/2,m})) \left\{ (-0.5 C_5 RR_{K,j}) + \frac{\bar{\rho}_o}{\bar{\rho}_{K+1/2,m}} \left( \frac{B}{2 + A_1 (P_{K+1,m} + P_{K,m})} \right) \right. \\
&+ \left( \frac{1}{2 H_{om} \bar{\rho}_{K+1/2,m}} \right) \left( \frac{B}{2 + A_1 (P_{K+1,m} + P_{K,m})} \right) (I_{K+1,m} + I_{K,m}) \\
&- \left( \frac{1}{2 H_{om} \bar{\rho}_{K+1/2,m}} \right) \left[ \left( \frac{H_{om} + \bar{f}_{K,m}}{\Delta T_m} + \frac{\bar{f}_{K,m}}{\Delta X_K} \right) \left( \frac{B}{2 + A_1 (P_{K+1,m} + P_{K,m})} \right) (\Delta X_K) \right. \\
&\left. \left. + \left( \frac{H_{om} + \bar{f}_{K+1,m}}{\Delta T_m} + \frac{\bar{f}_{K+1,m}}{\Delta X_K} \right) \left( \frac{B}{2 + A_1 (P_{K+1,m} + P_{K,m})} \right) (\Delta X_{K+1}) \right] \right\} \quad (D-11)
\end{aligned}$$

where

$$\delta_g = 1 \quad j = K+1$$

$$\delta_g = -1 \quad j = K$$

Eq. (D-11) is one of  $N \times N$  matrix elements, the expanded form of



Eq. (50) is

$$\begin{bmatrix}
 \frac{\partial \Psi_m(P_{KA})}{\partial P_{KA,m}} & \frac{\partial \Psi_m(P_{KA})}{\partial P_{KA+1,m}} & \dots & \frac{\partial \Psi_m(P_{KA})}{\partial P_{KO-1,m}} \\
 \frac{\partial \Psi_m(P_{KA+1})}{\partial P_{KA,m}} & \frac{\partial \Psi_m(P_{KA+1})}{\partial P_{KA+1,m}} & \dots & \frac{\partial \Psi_m(P_{KA+1})}{\partial P_{KO-1,m}} \\
 \vdots & \vdots & \ddots & \vdots \\
 \frac{\partial \Psi_m(P_{KO-1})}{\partial P_{KA,m}} & \frac{\partial \Psi_m(P_{KO-1})}{\partial P_{KA+1,m}} & \dots & \frac{\partial \Psi_m(P_{KO-1})}{\partial P_{KO-1,m}}
 \end{bmatrix}
 \begin{bmatrix}
 \Delta P_{KA,m} \\
 \Delta P_{KA+1,m} \\
 \vdots \\
 \Delta P_{KO-1,m}
 \end{bmatrix}
 = -
 \begin{bmatrix}
 \Psi_m(P_{KA}) \\
 \Psi_m(P_{KA+1}) \\
 \vdots \\
 \Psi_m(P_{KO-1})
 \end{bmatrix}$$

The inversion of the above square matrix is obtained by the Gaussian elimination method.  $\{\Delta P_{K,m}\}$  is the column matrix and added to  $\{P_{K,m}\}$  at each iteration. When  $\{\Delta P_{K,m}\}$  does not meet the convergence criteria, the iteration is repeated with the adjust inlet pressure by linear interpolation and a constant center pressure until the converged solution is obtained.



APPENDIX C

COMPUTER PROGRAM FLOW DIAGRAM AND FORTRAN LISTINGS

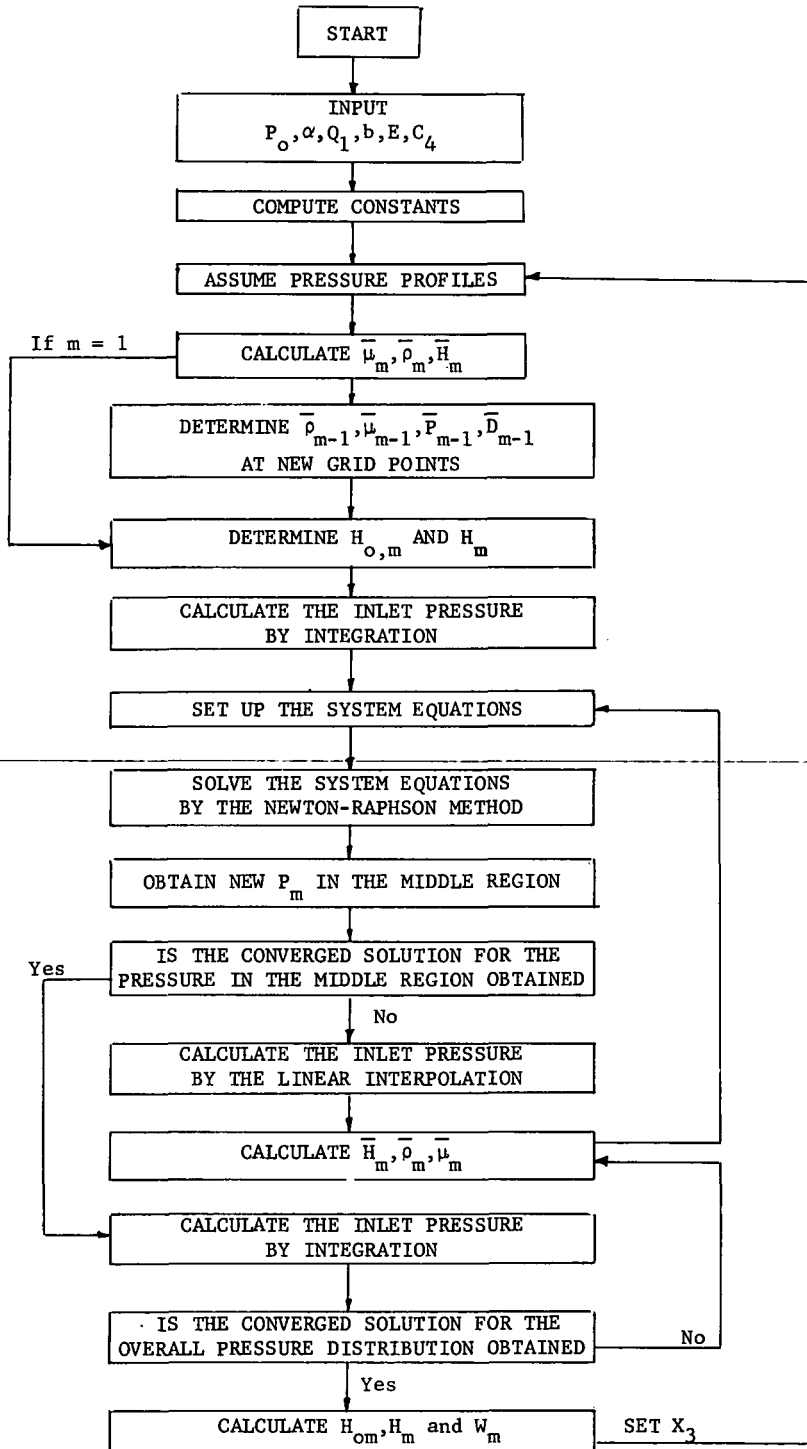


Fig. B-1. Flow Diagram For Program  
NASA 2.



```

PROGRAM NASA2(INPUT,OUTPUT,PUNCH,TAPE3,TAPE5=INPUT,TAPE6=OUTPUT)
COMMON KI,KO,KB,KBF,KF,MI,MF,KH,KKI,K2,KKO,KKB,KO2,KKF,KF2,
1K3,MMI,KKH,KBI,KBFF,IS,N,NN,XH,U2,PO,C2,RC,X3,PC,ALPH,E,PII,
2P1,H,HH,P,DEN,DEND,VIS,VISD,DE1,H1,PAI,VD,PSI,PSD,PS,DENX,C,
3KW,I,J,K,XC,KB2,KB1,EN,ED,PH,M,EE,SUBV,KIB,KIBF,C1,DX,S,IIS,
4KA,S1,H0,DT,U1,R,Q,D,DP,DENT,C9,BET,D1,NCT,C3,C4,U,DEO,C6,SOE,
5PT,PP,S3,S4
  DIMENSION XH(65),R(40,40),EE(40),H(57),H1(57),HH(57),P(65),
1P1(57),DEN(57),DEND(57),SOE(57),PAI(57),VIS(57),VISD(57),
2D(57),PS(57),DX(57),DP(57),VD(57),A(57),S(57),Q(57,65),
3DE1(57),HO(21),SUBV(65),F(65),C(2,3,65),BET(40,40),D1(57),
4PP(57),PT(57)
  DIMENSION TEM(40), NI(40,4)
  REWIND 3
  READ(5,100) KA, KO, KIB, KIBF, KF, MI, MF, KH
  READ(5,101) H3,PO,C5
  READ(5,103) PE, EU, EP, PC
  READ(5,108) E, EN, ED, ALPH
  KB=KIB $ KBF=KIBF
  PH=PO/E
  S4=1.1 $ S3=0.9
  KO=57 $ KF=65
  G=ALPH*336.0 $ KI=1
  PII=3.141593
  U=(H3*0.75/(1.26*G**0.6*PH**(-0.27)))**(10./7.)
  HO(1)=H3
  P(KI)=0.0 $ DEN(KI)=1.0 $ VIS(KI)=1.0
  C9=1.0/8.0 $ C3=16.0*PH**2 $ C4=C3/PII
  U1=48.0*U/(HO(1)**2) $ C1=C3/HO(1) $ C2=C1/PII
  C6=C5/C9**2
  XC=C6/H3
  WRITE(6,11) PH,E,EN,ED,ALPH
  WRITE(6,12) U,G,H3,U1,C1,C2
  WRITE(6,13) PO,C5
  HTM=HO(1)
  KKI=KI+1 $ K2=KI+2 $ KKO=KO+1 $ KKB=KB+1
  KO2=KO-2 $ KKF=KF-1 $ KF2=KF-2 $ K3=KI+3
  KA1=KA-1 $ KKA=KA+1
  MMI=MI+1 $ KKH=KH+1
  KO1=KO-1
  QKO=(1.0-1.0/EXP(ALPH))/ALPH
  XH(KI)=-4.0 $ DT=1.0/16.0
C   DETERMINE GRID SPACING AT FIRST TIME STEP.
  DO 7 K=2, 7
7   XH(K)=XH(K-1)+1.0/4.0
  DO 6 K=8, 13
6   XH(K)=XH(K-1)+1.0/8.0
  XH(KO)=0.0
C   DETERMINE PRESSURE DISTRIBUTION IN THE SECOND HALF OF CONTACT RE
C   -GION BASED ON THE HERTZIAN PROFILE.
  DO 202 K=KKO, KF

```



```

202 XH(K)=XH(K-1)+1.0/8.0
DO 201 K=KO, KF
201 P(K)=SQRT(1.0-(XH(K)**2))
WRITE(6,210) (K, P(K), K=KO, KF)
IIS=2 $ IS=1 $ P(KO)=1.0 $ K=KO $ CALL DHD $ DEO=DEN(KO)
NCS=1
NCT=1
IF(NCT.EQ.1) 175, 176
C READ DEFORMATION, DENSITY, PRESSURE OF PREVIOUS TIME STEP.
175 READ(5,623) (D1(K),K=KI,KO)
READ(5,623) (P1(K),K=KI,KO)
READ(5,623) (DE1(K),K=KI,KO)
READ(5,623) (PT(K),K=KI,KO)
READ(5,624) HO(15),C1,U1,XC
READ(5,624) HO(16),C1,U1,XC
C2=C1/PII
WRITE(6,110) U1,HO(1),C1,C2,XC
WRITE(6,668) (K,D1(K),K=KI,KO)
WRITE(6,668) (K,DE1(K),K=KI,KO)
WRITE(6,668) (K,P1(K),K=KI,KO)
DO 1714 I=1,16
1714 READ(3) M, ((Q(K,J),J=KI,KF),K=KI,KO)
176 DO 200 M=17,20
LL=0 $ IO=0 $ LC=0
IF(M.LE.2) 561, 562
C DETERMINATION OF DIVIDING POINT BETWEEN THE INLET AND
C MIDDLE REGION, THIS POINT DEPENDS UPON THE LOCATION OF
C ASPERITY AT EACH TIME STEP.
561 KA=39 $ GO TO 570
562 IF(M.LE.4) 563, 564
563 KA=39 $ GO TO 570
564 IF(M.EQ.5) 565, 566
565 KA=37 $ GO TO 570
566 IF(M.EQ.6) 567, 568
567 KA=35 $ GO TO 570
568 IF(M.EQ.7) 569, 571
569 KA=31 $ GO TO 570
571 IF(M.EQ.8) 572, 573
572 KA=33 $ GO TO 570
573 IF(M.EQ.9) 574, 575
574 KA=28 $ GO TO 570
575 IF(M.LE.12) 576,577
576 KA=27 $ GO TO 570
577 KA=25
570 IF(M.GE.18) 140, 141
140 KO=57 $ KF=65 $ KKF=KF-1 $ KKO=KO+1 $ KF2=KF-2
KO2=KO-2 $ KO1=KO-1
DO 142 K=KO, KF
142 P(K)=SQRT(1.0-(XH(K)**2))
141 CALL TRANS
KBI=KB+4 $ KBFF=KB+20
C READ THE KERNEL OF DEFORMATION FORMULA WHICH WERE
C CALCULATED AND STORED IN MAGNETIC TAPE.

```



```

      READ(3) M , ((Q(K,J), J=KI, KF), K=KI, KO)
      WRITE(6,100) M
      WRITE(6,15) KBI,KBF
      WRITE(6,603) ((K,J,Q(K,J),J=45,65),K=45,57)
      WRITE(6,668) (K, XH(K), K=KI, KO)
      WRITE(6,668) (K,DX(K),K=KI,KO)
      WRITE(6,100) KBI, KBF
      IF(M.EQ.1) 65, 66
65  P(KA)=0.35
      P(35)=0.08
      DO 61 K=35, 41
61  P(K)=P(KA)-(P(KA)-P(35))*(XH(KA)-XH(K))/(XH(KA)-XH(35))
      SCC=XH(35)-XH(1)
      DO 67 K=1,35
67  P(K)=P(35)-(XH(35)-XH(K))*P(35)/SCC
      KA1=KA-1
      KCA=KO-KA+1
      DO 586 K=KI,KO
586 PAI(K)=0.0
      DO 583 K=KI,KCA
      DO 583 J=KI,KCA
583 LET(K,J)=0.0
      PIP=1.0-P(KA1)
      DO 584 K=KA,KO
584 P(K)=P(KA1)+PIP*SQRT(1.0-(XH(K)/XH(KA))**2)
      CALL INTEG1(XH(KI),XH(KF),2,P,KF,VALUE,IER)
      IS=2$ IIS=2 $ CALL DHD
      GO TO 37
66  DO 174 K=KI,KO
      DEN(K)=DE1(K)
174 H1(K)=1.0+C1*0.5*XH(K)**2+D1(K)
      DO 156 K=KI, KO
      IF(K.GE.KBI.AND.K.LE.KBFF) 157, 158
157 H(K)=H1(K) $ HH(K)=H1(K)+XC*((ABS(X3-XH(K)))**2-C9**2)
      GO TO 159
158 H(K)=H1(K) $ HH(K)=H1(K)
159 P(K)=P1(K)
156 CONTINUE
273 WRITE(6,668) (K,DE1(K),K=KI,KO)
      WRITE(6,668) (K, H1(K), K=KI, KO)
      IF(M.LE.2) GO TO 522
      HO(M)=HO(M-1)*2.0-HO(M-2)
      WRITE(6,126) HO(M)$ GO TO 523
522 HO(M)=HO(M-1)
523 PKA=P(KA)
      CALL INTEG1(XH(KI),XH(KF),2,P,KF,VALUE,IER)
C    CALCULATION OF CENTER FILM THICKNESS.
      IF(M.GT.3) 186, 187
186 CMX=1.0E-20 $ HDEL=HO(M)*0.00005
      HMAX=HO(M)*(1.0+0.5)
      HMIN=HO(M)*(1.0-0.5)
      MT=15 $ HOI=HO(M)
C    NRONE SUBROUTINE DETERMINES CENTER FILM THICKNESS
C    AT FIRST TIME STEP.
      CALL NRONE(HO(M),CMX,MT,HDEL,HOI,HMAX,HMIN)

```



```

      U1=48.0*U/HO(M)**2 $ WRITE(6,110) U1, HO(M)
      IIS=1 $ CALL DHD $ CALL INTEG
      HOO=HO(M) $HTM=HO(M)
      IF(M.GE.3) GO TO 187
      S(KI)=0.0 $ KA1=KA-1
      DO 183 K=KI,KA
183  VD(K)=(H(K)-DEO/DEN(K)-PAI(K)/(DEN(K)*HO(M)))/HH(K)**3
      DO 184 K=KI,KA
      CALL INTEG2(XH(K),XH(K+1),1,VD,KO,VALUE,IER)
184  S(K+1)=S(K)+VALUE
      DO 185 K=KI,KA
      QK=U1*S(K)
185  P(K)=-ALOG(1.0-ALPH*QK)/ALPH
      WRITE(6,210) (K,P(K),K=KI,KA)
187  IF(M.GE.7) 341,112
341  PUNCH 623, (D1(K),K=KI,KO)
      PUNCH 623,(P1(K),K=KI,KO)
      PUNCH 623,(DE1(K),K=KI,KO)
      PUNCH 623, (PT(K),K=KI,KO)
      PUNCH 624, HO(M-1),C1,U1,XC
      GO TO 342
112  IF(M.GE.3) GO TO 109
      IF(NCT.EQ.2) GO TO 109
      IIS=2 $ IS=2 $ CALL DHD
      NC=KO-KA+1
      DO 278 K=KI,NC
      DO 278 J=KI,NC
278  BET(K,J)=0.0
      DO 279 K=KA,KO
279  PAI(K)=0.0
      PKA=P(KA)
      GO TO 264
342  PKA=P(KA)
      WRITE(6,210) (K,P(K),K=KI,KO)
      IIS=2 $ IS=2 $ CALL DHD $ IIS=1 $ CALL INTEG
      WRITE(6,642) (K,PAI(K), K=KI,KO)
      WRITE(6,213) (K,HH(K), K=KI, KO)
      WRITE(6,211) (K,H(K),K=KI,KO)
      JKA=(1.0-1.0/EXP(P(KA)*ALPH))/ALPH
      S(KI)=0.0 $ KA1=KA-1
      WRITE(6,642) (K,PAI(K),K=KA,KO)
      WRITE(6,110) U1,HO(M),C1,C2
      DO 645 K=KKI,KO1
645  PS(K)=P(K)
      GO TO 109
      DO 35 K=KI, KO
      PS(K)=P(K)
      PKA=P(KA)
      89 IF(IO+1.EQ.1) GO TO 109
144  MT=15 $ HOI=HO(M)
      LCC=2
      IF(M.EQ.1) 161, 162
C    CALCULATION OF CENTER FILM THICKNESS BASED ON THE
C    CORRECTED PRESSURE DISTRIBUTION BY NEWTON-RAPHSON METHOD.

```



```

161 CMX=1.0E-18 $ HDEL=HO(M)*0.00005
    HMAX=HO(M)*1.2
    HMIN=HO(M)*0.8
    GO TO 163
162 CMX=1.0E-21 $ HDEL=HO(M)*0.00005
    HMIN=HO(M)*0.5
    HMAX=HO(M)*1.5
163 CALL NRONE(HO(M),CMX,MT,HDEL,HOI,HMAX,HMIN)
    HCM=HO(M)
    HO(M)=(HTM+HO(M))*0.5
    HTM=HCM
    U1=48.0*U/HO(M)**2
    C1=C3/HO(M) $ C2=C1/PII $ XC=C6/HO(M)
    IIS=1 $ CALL DHD $ CALL INTEG
109 WRITE(6,110) HO(M),C1,C2,XC,U1
173 WRITE(6,110) HO(M),HO(M-1),DT,C3
    PKA=P(KA)
461 IS=2 $ IIS=2 $ CALL DHD
302 IF(M.EQ.1) 264, 263
263 IIS=2 $ CALL INTEG
264 IS=3$ CALL DHD
C  CALCULATION OF MATRIX ELEMENTS FO THE SYSTEM EQUATIONS.
    DO 90 K=KA, KO1
        N=K-KA+1
        SOE(K)=(H(K)+H(K+1))*0.5
        A(K)=(HH(K+1)+HH(K))*0.5
        C8=(P(K+1)-P(K))*(A(K)**2)/(VIS(K)*DX(K))
        IF(K.GE.KBI.AND.K.LE.KBFF) 411,412
411 STO=(S4-S3)*XC*(X3*XH(KBFF)-0.5*XH(KBFF)**2-X3*XH(K)
        X+0.5*XH(K)**2)
        GO TO 413
412 STO=0.0
413 EE(N)=C8*A(K)-U1*(0.5*(S4+S3)*(SOE(K)-DEO/DEN(K))-STO
        X-0.5/HO(M)*(PAI(K+1)+PAI(K))/DEN(K))
224 DO 90 J=KA,KO1
        II=J-KA+1
        QQ=0.0
521 IF(J.EQ.KA) 91, 92
    91 DO 93 I=KI, KA
    93 QQ=QQ+(Q(K,I)+Q(K+1,I))*P(I)/P(KA)
        GO TO 99
    92 QQ=Q(K,J)+Q(K+1,J)
    99 R(N,II)=-QQ*C2*(C8*1.5-0.25*(S4+S3)*U1)+0.5*U1/HO(M)*(BEI(N+1,
        XII)+BET(N,II))/DEN(K)
508 IF(J.EQ.K) GO TO 94
        IF(J.EQ.K+1) GO TO 95
        GO TO 90
    94 SIGN=-1.0 $ GO TO 98
    95 SIGN=1.0
    98 R(N,II)=R(N,II)+C8*A(K)*(SIGN/(P(K+1)-P(K))-VISD(K)/VIS(K))-
        X(U1*DEND(K)/DEN(K)**2)*(DEO*0.5*(S4+S3)+0.5/HO(M)*(PAI(K+1)
        X+PAI(K)))
    90 CONTINUE

```



```

280 IG=KO-KA
    IE=KO1-KA+1
    WRITE(6,110) C2, DEO, U1
C    SUBROUTINE IN1SP IS THE OPERATION OF MATRIX INVERSION.
    CALL IN1SP(R,IG,1.E-7,IEER, 40, TEM,NI)
    IF(IEER) 153,153,154
154 WRITE(6,100) IEER
    GO TO 1000
153 DO 105 N=KI,IG
    AS=0.0
    DO 106 II=KI,IE
106 AS=AS+R(N,II)*EE(II)
    K=N+KA-1
    DP(K)=-AS
    P(K)=P(K)+DP(K)
    PS(K)=P(K)
    IF(ABS(DP(K))-0.6) 105, 105, 503
105 CONTINUE
    WRITE(6,621) (K, DP(K),K=KA,KO1)
    GO TO 504
503 WRITE(6,621) (J,DP(J),J=KA,K) $ GO TO 1000
504 WRITE(6,100) LL, IO
    PKA=P(KA)
    PW=0.0 $ PQ=0.0
    DO 171 K=KA, KO1
    PW=PW+DP(K)
    PQ=PQ+P(K)
171 CONTINUE
    PQR=ABS(PW/PQ)
    KA1=KA-1
    LL=LL+1
128 IF(PQR.LE.0.0005) 166, 48
    48 IF(LL.LE.10) 301, 322
301 DO 402 K=KI,KA1
    P(K)=P(K)*P(KA)/PKA
402 PS(K)=P(K)
547 PKA=P(KA)
    GO TO 461
C    INLET PRESSURE CALCULATION BY INTEGRATION.
166 DO 241 K=KI,KO
    IF(K.GE.KBI.AND.K.LE.KBFF) 414, 415
414 STO=(S4-S3)*XC*(X3*XH(KBFF)-0.5*XH(KBFF)**2-X3*XH(K)+0.5*XH(K)*
    X*2)
    GO TO 241
415 STO=0.0
241 VD(K)=((S3+S4)*0.5*(H(K)-DEO/DEN(K))-STO-PAI(K)/(HO(M)*DEN(K)))
    X/HH(K)**3
    QKA=(1.0-1.0/EXP(ALPH*P(KA)))/ALPH
    S(KI)=0.0 $ KA1=KA-1
    DO 73 K=KI,KA
73 S(K+1)=S(K)+0.5*(VD(K)+VD(K+1))*DX(K)
    DO 75 K=KI,KA1
    P1(K)=QKA*S(K)/S(KA)
    QCC=ALPH*P1(K)
    IF(QCC) 532, 533, 533

```



```

532 WRITE(6,668) (K,S(K),K=KI,KA)
   WRITE(6,668) (K,VD(K),K=KI,KA)
   LCC=1 $ GO TO 534
533 IF(QCC.GE.1.0) 545, 75
545 WRITE(6,668) (K,VD(K),K=KI,KO)
   KA=K-1
   WRITE(6,100) KA
   LCC=1 $ GO TO 1000
75 CONTINUE
   DO 537 K=KI,KA1
537 P(K)=-ALOG(1.0-ALPH*P1(K))/ALPH
   GO TO 322
C   THE CALCULATION OF INLET PRESSURE BY THE LINEAR INTERPOLATION
C   WHEN THE CONVERGED SOLUTION IS NOT OBTAINED FOR THE
C   PRESSURE IN THE MIDDLE REGION.
534 DO 536 K=KI,KA1
536 P(K)=P(K)*P(KA)/PKA
   PKA=P(KA)
322 PW=0.0 $ PQ=0.0
C   THE OVERALL CONVERGENCE TEST.
   DO 113 K=KKI,KO1
   PQ=PQ+P(K)-PS(K)
113 PW=PW+P(K)
   LL=0 $ PQR=ABS(PQ/PW)
   IF(PQR.LE.0.0005) 651, 115
115 IO=IO+1
   IF(IO.LE.10) 49, 651
49 DO 116 K=KKI, KO1
116 PS(K)=P(K)
   IIS=2 $ IS=2 $ CALL DHD $ IIS=1 $ CALL INTEG
   LC=0
   GO TO 144
114 IF(IO.LE.1) GO TO 109
   DHC=(HOO-HO(M))/HO(M)
   IF(ABS(DHC).LE.0.002) 651, 652
652 HOO=HO(M) $ GO TO 109
651 CALL INTEG2(XH(KI),XH(KF),2,P,KF,VALUE,IER)
   W=VALUE
   C1=C3/HO(M) $ C2=C1/PI1 $ IIS=2 $ IS=2 $ CALL DHD
   HTM=HO(M)
   WS=W*4.0*(PH**2)
C   CALCULATION OF THE CENTER FILM THICKNESS BY THE
C   NEW PRESSURE DISTRIBUTION.
   CALL NRONE(HO(M),CMX,MT,HDEL,HOI,HMAX,HMIN)
   U1=48.0XU/HO(M)**2
   WRITE(6,220) M, W, HO(M)
   WRITE(6,210) (K, P(K), K=KI, KO)
   WRITE(6,213) (K, HH(K), K=KI, KO)
   WRITE(6,211) (K, H(K), K=KI, KO)
   WRITE(6,215) (K, D(K), K=KI, KO)
   WRITE(6,126) WS
   WRITE(6,642) (K,PAI(K), K=KI,KO)
   WRITE(6,643) C1,C2,HO(M)
   DO 580 K=KI, KO

```



```

580 HH(K)=HH(K)*HO(M)
    WRITE(6,213) (K,HH(K),K=KI,KO)
    IF(M.EQ.1) 452, 453
452 DO 454 K=KI,KO
454 PP(K)=P(K)
    GO TO 456
453 DO 451 K=KI,KO
    PS(K)=P(K)-PT(K)
451 PP(K)=PT(K)
    WRITE(6,626) (K,PS(K),K=KI,KO)
456 DO 182 K=KI,KO1
    SM=P(K)-1.05
    IF(SM)182, 182, 1000
182 CONTINUE
    IF(M.LE.8) 200, 218
218 WRITE(6,601) M,WS,HO(M)
200 CONTINUE
1000 STOP
    11 FORMAT(5H PH=,E14.6,3H E=,E14.6,4H EN=,E14.6,4H U1=,E14.6,
        X6H ALPHA=,E14.6)
    12 FORMAT(5H U=,E14.6,3H G=,E14.6,4H H3=,E14.6,4H U1=,E14.6,
        X4H C1=,E14.6,4H C2=,E14.6)
    13 FORMAT(6H PO=,E14.6,4H C5=,E14.6)
    15 FORMAT(6H KBI=,I3,6H KBF=, I3)
100 FORMAT(8I5)
101 FORMAT(E10.1,F10.1,E10.1)
103 FORMAT(4E10.1)
104 FORMAT(F10.1, E10.1, E10.1, E10.2, F5.2)
108 FORMAT(3E10.2, F5.1)
110 FORMAT(6E15.8)
126 FORMAT(6E15.6, 2I5)
213 FORMAT(3X//50X, *HH(K,M)=*//2X,*K*,20X,*K*,20X,*K*,
    X20X,*K*,20X,*K*,20X,*K*//((6(I3,E15.7,3X)))
210 FORMAT(3X//50X, *P(K,M)=*//2X, *K*, 20X, *K*, 20X, *K*,
    X20X, *K*, 20X, *K*,20X, *K*//((6(I3, E15.7, 3X)))
211 FORMAT(3X//50X, *H(K,M)=*//2X, *K*, 20X, *K*, 20X, *K*,
    X20X, *K*, 20X, *K*,20X, *K*//((6(I3, E15.7, 3X)))
214 FORMAT(10H SOE(K)=*//((6(I4,2X,E15.7)))
212 FORMAT(5H C8=,E12.5,7H EE(K)=,E12.5,8H VIS(K)=,E12.5
    X,8H DEN(K)=,E12.5)
226 FORMAT(5H CC=,E12.5,6H ROLL=,E12.5,4H SQ=,E12.5,5H SUM=,E12.5)
227 FORMAT(6H A(K)=,E12.5,8H PAI(K)=,E12.5,8H SOE(K)=,E12.5)
215 FORMAT(3X//50X, *D(K,M)=*//2X, *K*, 20X, *K*, 20X, *K*,
    X20X, *K*, 20X, *K*,20X, *K*//((6(I3, E15.7, 3X)))
668 FORMAT(2X//((6(I4, 1X, E16.8)))
601 FORMAT(4H M=,I3,6H WS=,E15.7,7H HO(M)=,E15.7)
603 FORMAT(3X//50X, *MATRIX R(K,J)*//((5(2I4, E14.5)))
220 FORMAT(1H1, 2X, *M=*, I3, 4X, *W(M)=*, E15.8, 4X, *HO(M)=*, E15.8)
621 FORMAT(/3X,*DP(K)=*//((6(I4,1X,E16.8)))
623 FORMAT(6E12.5)
624 FORMAT(4E20.10)
626 FORMAT(3X//40X,*THE PRESSURE DIFFERENCE*//2X,*K*,20X,*K*,
    X20X,*K*,20X,*K*,20X,*K*,20X,*K*//((6(I3,E15.7,3X)))
632 FORMAT(/3X,*EE(K)=*//((6(I4,2X,E15.7)))

```



```

637 FORMAT(/3X,*DEN(K)=*// (6(I4,2X,E15.7)))
642 FORMAT(/3X,*PAI(K)=*// (6(I4,1X,E15.7)))
643 FORMAT(5H C1=,E15.6,5H C2=,E15.6,8H HO(M)=,E15.6)
END
SUBROUTINE TRANS
C THE CALCULATION OF NEW GRID SPACINGS AND DETERMINATION
C OF PRESSURE, DENSITY, DEFORMATION AT NEW GRID POINTS.
COMMON KI,KO,KB,KBF,KF,MI,MF,KH,KKI,K2,KKO,KKB,KO2,KKF,KF2,
1K3,MMI,KKH,KDI,KBFF,IS,N,NN,XH,U2,P0,C2,RC,X3,PC,ALPH,E,PII,
2P1,H,HH,P,DEN,DEND,VIS,VISD,DE1,H1,PAI,VD,PSI,PSD,PS,DENX,C,
3KW,I,J,K,XC,KB2,KB1,EN,ED,PH,M,EE,SUBV,KIB,KIBF,C1,DX,S,IIS,
4KA,S1,HO,DT,U1,R,Q,D,DP,DENT,C9,BET,D1,NCT,C3,C4,U,DEO,C6,SOE,
5PT,PP,S3,S4
DIMENSION XH(65),R(40,40),EE(40),H(57),H1(57),HH(57),P(65),
1P1(57),DEN(57),DEND(57),SOE(57),PAI(57),VIS(57),VISD(57),
2D(57),PS(57),DX(57),DP(57),VD(57),A(57),S(57),Q(57,65),
3DE1(57),HO(21),SUBV(65),F(65),C(2,3,65),BET(40,40),D1(57),
4PP(57),PT(57)
MM=M
KKK=0 $ KO1=KO-1
IF(MM.EQ.1) 55, 58
58 L=MM/2 $ IF(MM.EQ.L*2) 81, 82
81 KB=KIB+M $ KBF=KIBF+M-1 $ KKK=1
KBC=KB-2
IF(MM.EQ.2) 71, 72
71 XH(14)=XH(13)+1.0/32.0
XH(KB)=XH(14)+1.0/32.0
GO TO 55
72 DO 73 K=14, KBC
73 XH(K)=XH(K-1)+1.0/16.0
XH(KBC+1)=XH(KBC)+1.0/32.0
XH(KB)=XH(KB-1)+1.0/32.0
GO TO 55
82 KB=KIB+M-1 $ KBF=KIBF+M-1 $ KKK=0
DO 74 K=14, KB
74 XH(K)=XH(K-1)+1.0/16.0
GO TO 55
55 KKB=KB+1 $ KB20=KB+20 $ KKBF=KBF+1
DO 12 K=KKB, KB20
IF(K.LE.KB+4) 16, 18
16 XH(K)=XH(K-1)+1.0/32.0
GO TO 12
18 XH(K)=XH(K-1)+1.0/64.0
12 CONTINUE
IF(KKK.EQ.1) 24, 25
24 XH(KB+21)=XH(KB+20)+1.0/32.0
XH(KB+22)=XH(KB+21)+1.0/32.0
XH(KBF)=XH(KB+22)+1.0/16.0
GO TO 56
25 KB21=KB+21
DO 26 K=KB21, KBF
26 XH(K)=XH(K-1)+1.0/32.0
56 CONTINUE

```



```

94 DO 96 K=KKBF, KO
96 XH(K)=XH(K-1)+1.0/16.0
DO 97 K=KKO, KF
97 XH(K)=XH(K-1)+1.0/8.0
78 X3=XH(KB+12)
DO 234 K=KI, KO1
234 DX(K)=XH(K+1)-XH(K)
113 KB1=KB-1 $ KB2=KB+2 $ KBF1=KBF-1
KB4=KB+4 $ KB16=KB+16 $ KB17=KB+17 $ KB20=KB+20
KB21=KB+21
IF(NCT.EQ.1.AND.M.LE.17) 63,64
64 IF(M.EQ.1) GO TO 63
225 DO 67 K=KI, KO
IF(K.LE.KB-2. OR. K. GE. KBF) 68, 67
68 DE1(K)=DEN(K)$P1(K)=P(K)$D1(K)=D(K)$PT(K)=PP(K)
67 CONTINUE
230 L=M/2 $ IF(M.EQ.2*L) 201, 202
201 DO 203 K=KB1, KB2
DE1(K)=DEN(K) $ P1(K)=P(K)
PT(K)=PP(K)
203 D1(K)=D(K)
DE1(KB+3)=DE1(KB+4) $ D1(KB+3)=D(KB+4)
PT(KB+3)=PP(KB+3)
P1(KB+3)=P(KB+3)
DO 204 K=KB4, KB16
DE1(K)=DEN(K+2) $ D1(K)=D(K+2)
PT(K)=PP(K+2)
204 P1(K)=P(K+2)
DO 205 K=KB17, KB20
IF(K.EQ.KB20) 219, 220
220 L=K/2 $ IF(K.EQ.2*L) 217, 218
217 IF(K.EQ.KB17) 302, 303
302 DE1(K)=DEN(K+1)+0.5*(DEN(K+2)-DEN(K+1))
D1(K)=D(K+1)+0.5*(D(K+2)-D(K+1))
PT(K)=PP(K+1)+0.5*(PP(K+2)-PP(K+1))
P1(K)=P(K+1)+0.5*(P(K+2)-P(K+1))
GO TO 205
303 DE1(K)=DEN(K)+0.5*(DEN(K+1)-DEN(K))
D1(K)=D(K)+0.5*(D(K+1)-D(K))
PT(K)=PP(K)+0.5*(PP(K+1)-PP(K))
P1(K)=P(K)+0.5*(P(K+1)-P(K))
GO TO 205
218 DE1(K)=DEN(K+1) $ D1(K)=D(K+1)
PT(K)=PP(K+1)
P1(K)=P(K+1)
GO TO 205
219 DE1(K)=DEN(K) $ D1(K)=D(K)
PT(K)=PP(K)
P1(K)=P(K)
205 CONTINUE
DO 206 K=KB21, KBF1
DE1(K)=DEN(K) $ D1(K)=D(K)
PT(K)=PP(K)
206 P1(K)=P(K)
GO TO 63

```



```

202 DE1(KB1)=DEN(KB)
   PT(KB1)=PP(KB)
   D1(KB1)=D(KB) $ P1(KB1)=P(KB)
   DO 208 K=KB, KBF1
   IF(K.LE.KB+2) 209, 210
209 DE1(K)=DEN(K+2) $D1(K)=D(K+2)
   PT(K)=PP(K+2)
   P1(K)=P(K+2)
   GO TO 208
210 IF(K.LT.KB+4) 211, 212
211 DE1(K)=DEN(K+2)
   D1(K)=D(K+2)
   PT(K)=PP(K+2)
   P1(K)=P(K+2)
   GO TO 208
212 IF(K.LE.KB+16) 213, 214
213 DE1(K)=DEN(K+4)
   D1(K)=D(K+4)
   PT(K)=PP(K+4)
   P1(K)=P(K+4)
   GO TO 208
214 IF(K.LE.KB+20) 215, 216
215 L=K/2 $ IF(K.EQ.2*L)221, 222
221 IF(K.EQ.KB+17) 281, 282
281 DE1(K)=DEN(K+3)+0.5*(DEN(K+4)-DEN(K+3))
   D1(K)=D(K+3)+0.5*(D(K+4)-D(K+3))
   PT(K)=PP(K+3)+0.5*(PP(K+4)-PP(K+3))
   P1(K)=P(K+3)+0.5*(P(K+4)-P(K+3))
   GO TO 208
282 DE1(K)=DEN(K+2)+0.5*(DEN(K+3)-DEN(K+2))
   D1(K)=D(K+2)+0.5*(D(K+3)-D(K+2))
   PT(K)=PP(K+2)+0.5*(PP(K+3)-PP(K+2))
   P1(K)=P(K+2)+0.5*(P(K+3)-P(K+2))
   GO TO 208
222 IF(K.EQ.KB+18) 284, 285
284 DE1(K)=DEN(K+3)$D1(K)=D(K+3)$P1(K)=P(K+3)$PT(K)=PP(K+3)$GO TO 208
285 DE1(K)=DEN(K+2)$D1(K)=D(K+2)$P1(K)=P(K+2)$PT(K)=PP(K+2)$GO TO 208
216 L=K/2 $ IF(K.EQ.2*L) 223, 224
223 IF(K.EQ.KB+21) 286, 287
286 DE1(K)=DEN(K+1)+0.5*(DEN(K+2)-DEN(K+1))
   D1(K)=D(K+1)+0.5*(D(K+2)-D(K+1))
   PT(K)=PP(K+1)+0.5*(PP(K+2)-PP(K+1))
   P1(K)=P(K+1)+0.5*(P(K+2)-P(K+1))
   GO TO 208
287 DE1(K)=DEN(K)+0.5*(DEN(K+1)-DEN(K))
   D1(K)=D(K)+0.5*(D(K+1)-D(K))
   PT(K)=PP(K)+0.5*(PP(K+1)-PP(K))
   P1(K)=P(K)+0.5*(P(K+1)-P(K))
   GO TO 208
224 DE1(K)=DE1(K+1)
   D1(K)=D(K+1)
   PT(K)=PP(K+1)
   P1(K)=P(K+1)
208 CONTINUE
63 CONTINUE

```



```

RETURN
END
SUBROUTINE DHD
C THE CALCULATION OF FILM THICKNESS, DENSITY AND VISCOSITY.
COMMON KI,KO,KB,KBF,KF,MI,MF,KH,KKI,K2,KKO,KKB,KO2,KKF,KF2,
1K3,MMI,KKH,KBI,KBFF,IS,N,NN,XH,U2,PO,C2,RC,X3,PC,ALPH,E,PII,
2P1,H,HH,P,DEN,DEND,VIS,VISD,DE1,H1,PAI,VD,PSI,PSD,PS,DENX,C,
3KW,I,J,K,XC,KB2,KBI,EN,ED,PH,M,EE,SUBV,KIB,KIBF,C1,DX,S,IIS,
4KA,S1,HO,DT,U1,R,Q,D,DP,DENT,C9,BET,D1,NCT,C3,C4,U,DEO,C6,SOE,
5PT,PP,S3,S4
DIMENSION XH(65),R(40,40),EE(40),H(57),H1(57),HH(57),P(65),
1P1(57),DEN(57),DEND(57),SOE(57),PAI(57),VIS(57),VISD(57),
2D(57),PS(57),DX(57),DP(57),VD(57),A(57),S(57),Q(57,65),
3DE1(57),HO(21),SUBV(65),F(65),C(2,3,65),BET(40,40),D1(57),
4PP(57),PT(57)
IF(IIS,EQ.1) 18, 41
41 IF(IS-2) 10,11, 12
10 DEN(K)=1.0+EN*P(K)/(1.0+ED*P(K))
DEND(K)=EN/((1.0+P(K)*ED)**2)
VIS(K)=EXP(ALPH*P(K))
VISD(K)=ALPH*VIS(K)
GO TO 25
11 DO 13 K=KI, KO
DEN(K)=1.0+EN*P(K)/(1.0+ED*P(K))
DEND(K)=EN/((1.0+P(K)*ED)**2)
VIS(K)=EXP(ALPH*P(K))
VISD(K)=ALPH*VIS(K)
13 CONTINUE
GO TO 18
12 DO 20 K=KA, KO
P4=(P(K+1)+P(K))*0.5
DEN(K)=1.0+EN*P4/(1.0+ED*P4)
DEND(K)=0.5*EN/((1.0+ED*P4)**2)
VIS(K)=EXP(ALPH*P4)
VISD(K)=0.5*ALPH*VIS(K)
20 CONTINUE
18 DO 14 K=KI, KO
DS=0.0
DO 15 J=KI, KF
15 DS=DS+Q(K,J)*P(J)
D(K)=-C2*DS
H(K)=1.0+C1*0.5*(XH(K)**2)+D(K)
IF(K.GE.KBI.AND.K.LE.KBFF) 31, 32
31 HH(K)=H(K)+XC*((ABS(X3-XH(K)))**2-C9**2) $ GO TO 14
32 HH(K)=H(K)
14 CONTINUE
25 CONTINUE
RETURN
END
SUBROUTINE INTEG1 (A,B,KCT,F,NP,VALUE,IERR)
C THE CALCULATION OF INTEGRALS BY THE OVERLAPPING PARABOLA
C FORMULA.

```



```

COMMON KI,KO,KB,KBF,KF,MI,MF,KH,KKI,K2,KKO,KKB,KO2,KKF,KF2,
1K3,MMI,KKH,KBI,KBFF,IS,N,NN,XH,U2,PO,C2,RC,X3,PC,ALPH,E,PII,
2P1,H,HH,P,DEN,DEND,VIS,VISD,DE1,H1,PAI,VD,PS1,PSD,PS,DENX,C,
3KW,I,J,K,XC,KB2,KBI,EN,ED,PH,M,EE,SUBV,KIB,KIBF,C1,DX,S,IIS,
4KA,S1,HO,DT,U1,R,Q,D,DP,DENT,C9,BET,D1,NCT,C3,C4,U,DEO,C6,SOE,
5PT,PP,S3,S4
  DIMENSION XH(65),R(40,40),EE(40),H(57),H1(57),HH(57),P(65),
1P1(57),DEN(57),DEND(57),SOE(57),PAI(57),VIS(57),VISD(57),
2D(57),PS(57),DX(57),DP(57),VD(57),A(57),S(57),Q(57,65),
3DE1(57),HO(21),SUBV(65),F(65),C(2,3,65),BET(40,40),D1(57),
4PP(57),PT(57)
  IF (NP.LE.3) GO TO 96
*   CALCULATION OF INTERVALS OF X
  NH=NP-1
  DO 10 I=1,NH
10  DX(I)=XH(I+1)-XH(I)
  DO 20 I=1, NH
*   DEFINE COEFFICIENTS OF FIRST PARABOLA
  IF(I.EQ.1) GO TO 15
  C(1,1,I)=-DX(I)**3/(6.0*DX(I-1)*(DX(I-1)+DX(I)))
  C(1,2,I)=DX(I)*(3.0*DX(I-1)+DX(I))/(6.0*DX(I-1))
  C(1,3,I)=DX(I)*(3.0*DX(I-1)+2.0*DX(I))/(6.0*(DX(I-1)+DX(I)))
15  CONTINUE
  IF(I.EQ.NH) GO TO 20
  C(2,1,I)=DX(I)*(2.0*DX(I)+3.0*DX(I+1))/(6.0*(DX(I)+DX(I+1)))
  C(2,2,I)=DX(I)*(DX(I)+3.0*DX(I+1))/(6.0*DX(I+1))
  C(2,3,I)=-DX(I)**3/(6.0*DX(I+1)*(DX(I)+DX(I+1)))
20  CONTINUE
  ENTRY INTEG2
  VALUE=0.0
  IF (B-A) 40,92,30
*   B IS GREATER THAN A
30  ALIM = A
  BLIM = B
  SIGN = 1.0
  GO TO 50
*   A IS GREATER THAN B
40  ALIM = B
  BLIM = A
  SIGN = -1.0
50  NH=NP-1
  IF(KCT.EQ.1) 125, 123
*   CALCULATION OF INTEGRAL OVER SUBINTERVAL
123 DO 80 I=1, NH
  SUBV(I)=0.0
  IF(XH(I).EQ.ALIM) SUBV(I)=C(2,1,I)*F(I)+C(2,2,I)*F(I+1)
  X+C(2,3,I)*F(I+2)
  IF(XH(I+1).EQ.BLIM) SUBV(I)=C(1,1,I)*F(I-1)+C(1,2,I)*F(I)
  X+C(1,3,I)*F(I+1)
  IF(XH(I).GT.ALIM.AND.XH(I+1).LT.BLIM) SUBV(I)=0.5*(C(1,1,I)
  X*F(I-1)+(C(1,2,I)+C(2,1,I))*F(I)+(C(1,3,I)+C(2,2,I))*F(I+1)+
  XC(2,3,I)*F(I+2))
80  VALUE=VALUE+SUBV(I)
  VALUE=SIGN*VALUE
  GO TO 92

```



```

125 DO 110 I=1, NH
    SUBV(I)=0.0
    IF(XH(I).EQ.ALIM) 111, 110
111 IF(I.EQ.NH) 113, 114
113 SUBV(I)=C(1,1,I)*F(I-1)+C(1,2,I)*F(I)+C(1,3,I)*F(I+1)
    GO TO 120
114 IF(I.GE.2) 115, 116
115 SUBV(I)=0.5*(C(1,1,I)*F(I-1)+(C(1,2,I)+C(2,1,I))*F(I)+(C(1,3,I)
    X+C(2,2,I))*F(I+1)+C(2,3,I)*F(I+2))
    GO TO 120
116 SUBV(I)=C(2,1,I)*F(I)+C(2,2,I)*F(I+1)+C(2,3,I)*F(I+2)
120 VALUE=SIGN*SUBV(I) $ GO TO 92
110 CONTINUE
*   SET ERROR PARAMETER FOR TOO FEW POINTS
    92 IERR = 0
    RETURN
*   SET ERROR PARAMETER FOR NORMAL RETURN
    96 IERR = 1
    RETURN
*   SET ERROR PARAMETER FOR A AND/OR B OUT OF RANGE OF TABLE
    97 IERR = 2
    RETURN
    END
    SUBROUTINE INTEG
C   THE CALCULATION OF (IX), THE INTEGRAL OF
C   SQUEEZING TERM.
    COMMON KI,KO,KB,KBF,KF,MI,MF,KH,KKI,K2,KKO,KKB,KO2,KKF,KF2,
    1K3,MMI,KKH,KBI,KBFF,IS,N,NN,XH,U2,PO,C2,RC,X3,PC,ALPH,E,PII,
    2P1,H,HH,P,DEN,DEND,VIS,VISD,DE1,H1,PAI,VD,PSI,PSD,PS,DENX,C,
    3KW,I,J,K,XC,KB2,KB1,EN,ED,PH,M,EE,SUBV,KIB,KIBF,C1,DX,S,IIS,
    4KA,S1,H0,DT,U1,R,Q,D,DP,DENT,C9,BET,D1,NCT,C3,C4,U,DEO,C6,SOE,
    5PT,PP,S3,S4
    DIMENSION XH(65),R(40,40),EE(40),H(57),H1(57),HH(57),P(65),
    1P1(57),DEN(57),DEND(57),SOE(57),PAI(57),VIS(57),VISD(57),
    2D(57),PS(57),DX(57),DP(57),VD(57),A(57),S(57),Q(57,65),
    3DE1(57),H0(21),SUBV(65),F(65),C(2,3,65),BET(40,40),D1(57),
    4PP(57),PT(57)
    IF(M.EQ.1) 81, 82
    81 DO 83 K=KI, KO
    83 PAI(K)=0.0 $ GO TO 86
    82 DO 60 K=KI, KO
        SD=(H0(M)*DEN(K)-H0(M-1)*DE1(K))/DT
202 IF(K.GE.KBI.AND.K.LT.KBFF) 61, 62
    61 DENT=(DEN(K)-DE1(K))/DT
        DENX=(DEN(K)-DEN(K-1))/DX(K-1)*0.5*(S4+S3)
        SE=XC*H0(M)*((ABS(X3-XH(K))**2-C9**2)*(DENT+DENX)
        SOE(K)=SD+SE
        GO TO 60
    62 SOE(K)=SD
    60 CONTINUE
    PAI(KO)=0.0
    KO1=KO-1
    DO 63 K=KI, KO1
        J=KO-K

```



```

63 PAI(J)=PAI(J+1)+0.5*DX(J)*(SOE(J)+SOE(J+1))
   IF(IIS.EQ.1) GO TO 86
   DO 101 K=KA,KO
   DO 101 J=KA, KO
   SSS=0.0 $ NN=K-KA+1 $ II=J-KA+1
   BET(NN,II)=0.0
   IF(K.EQ.KO) GO TO 161
   IF(K.GE.KBI.AND.K.LT.KBFF) 162,155
162 IF(J.GE.K) 154,155
154 IF(K.EQ.KBFF-1) 163,164
163 IF(J.EQ.K) 165, 155
165 BET(NN,II)=XC*HO(M)*((ABS(X3-XH(J)))**2-C9**2)*DEND(J)*
   X(0.5*(S4+S3)*DX(J)/DX(J-1)+DX(J)/DT)*0.5
   GO TO 155
164 BET(NN,II)=XC*HO(M)*((ABS(X3-XH(J)))**2-C9**2)
   X*DEND(J)*(0.5*(S4+S3)/DX(J-1)+1.0/DT)*(XH(J+1)-XH(J-1))*0.5
155 IF(J-K) 101, 107, 108
107 BET(NN,II)=0.5*DX(J)*DEND(J)*HO(M)/DT+BET(NN,II)
   GO TO 101
108 BET(NN,II)=0.5*DEND(J)*HO(M)*(XH(J+1)-XH(J-1))/DT+BET(NN,II)
   GO TO 101
161 BET(KO-KA+1,II)=0.0
101 CONTINUE
86 CONTINUE
   RETURN
203 FORMAT(4H FF=,E12.5,4H F2=,E12.5,4H F3=,E12.5,4H F4=,E12.5,
   X4H F5=,E12.5)
204 FORMAT(6HHO(M)=,E12.5,4H C3=,E12.5,6HXH(K)=,E12.5,7HDEN(K)=E12.5)
205 FORMAT(8HHO(M-1)=,E12.5,4H DD=,E12.5,6H DDD=,E12.5,7HDE1(K)=,
   XE12.5)
210 FORMAT(50X,*KERNEL=*//((5(2I4,E14.5)))
211 FORMAT(50X,*DEND(K)=*//((6(I4,1X,E15.7)))
212 FORMAT(50X,*DX(K)=*//((6(I4,1X,E15.7)))
   END
   FUNCTION PHI(SR)
C THE CALCULATION OF THE COEFFICIENTS OF EQUATION(54) OF PART II.
   COMMON KI,KO,KB,KBF,KF,MI,MF,KH,KKI,K2,KKO,KKB,KO2,KKF,KF2,
   1K3,MMI,KKH,KBI,KBFF,IS,N,NN,XH,U2,PO,C2,RC,X3,PC,ALPH,E,PII,
   2P1,H,HH,P,DEN,DEND,VIS,VISD,DE1,H1,PAI,VD,PSI,PSD,PS,DENX,C,
   3KW,I,J,K,XC,KB2,KBI,EN,ED,PH,M,EE,SUBV,KIB,KIBF,C1,DX,S,IIS,
   4KA,S1,HO,DT,U1,R,Q,D,DP,DENT,C9,BET,D1,NCT,C3,C4,U,DEO,C6,SOE,
   5PT,PP,S3,S4
   DIMENSION XH(65),R(40,40),EE(40),H(57),H1(57),HH(57),P(65),
   1P1(57),DEN(57),DEND(57),SOE(57),PAI(57),VIS(57),VISD(57),
   2D(57),PS(57),DX(57),DP(57),VD(57),A(57),S(57),Q(57,65),
   3DE1(57),HO(21),SUBV(65),F(65),C(2,3,65),BET(40,40),D1(57),
   4PP(57),PT(57)
   QKO=(1.0-1.0/EXP(ALPH))/ALPH
   C1=C3/SR $ C2=C1/PII $ XC=C6/SR
   IIS=1 $ CALL DHD $ CALL INTEG
   IF(M.EQ.1) 3, 4
3 DO 5 K=KI, KO
   IF(K.GE.KBI.AND.K.LE.KBFF) 20, 21

```



```

20 STO=(S4-S3)*XC*(X3*XH(KBFF)-0.5*XH(KBFF)**2-X3*XH(K)
   X+0.5*XH(K)**2) $ GO TO 5
21 STO=0.0
5 VD(K)=((S4+S3)*0.5*(H(K)-DEO/DEN(K))-STO)/(HH(K)**3)
  CALL INTEG2(XH(KI), XH(KO),2,VD,KO,VALUE,IER)
  S1=VALUE
n PHI=48.0*U/SR**2-(QKO/S1)
  GO TO 10
4 DO 2 K=KI, KO
  S(K)=PAI(K)/(HH(K)**3*DEN(K))
  IF(K.GE.KBI.AND.K.LE.KBFF) 22, 23
22 STO=(S4-S3)*XC*(X3*XH(KBFF)-0.5*XH(KBFF)**2-X3*XH(K)
   X+0.5*XH(K)**2) $ GO TO 2
23 STO=0.0
2 VD(K)=((S4+S3)*0.5*(H(K)-DEO/DEN(K))-STO)/(HH(K)**3)
  CALL INTEG2(XH(KI),XH(KO),2, VD,KO,VALUE,IER)
  S1=VALUE
  CALL INTEG2(XH(KI),XH(KO),2,S,KO,VALUE,IER)
  S2=VALUE
  PHI=QKO*SR**3-48.0*U*(S1*SR-S2)
10 RETURN
  END
  SUBROUTINE NRONE(X,CONV,NIT,DELXO, XO,XMAX,XMIN)
  COMMON KI,KO,KB,KBF,KF,MI,MF,KH,KKI,K2,KKO,KKB,KO2,KKF,KF2,
1K3,MMI,KKH,KBI,KBFF,IS,N,NN,XH,U2,PO,C2,RC,X3,PC,ALPH,E,PII,
2P1,H,HH,P,DEN,DEND,VIS,VISD,DE1,H1,PAI,VD,PSI,PSD,PS,DENX,C,
3KW,I,J,K,XC,KB2,KB1,EN,ED,PH,M,EE,SUBV,KIB,KIBF,C1,DX,S,IIS,
4KA,S1,HO,DT,U1,R,Q,D,DP,DENT,C9,BET,D1,NCT,C3,C4,U,DEO,C6,SOE,
5PT,PP,S3,S4
  DIMENSION XH(65),R(40,40),EE(40),H(57),H1(57),HH(57),P(65),
1P1(57),DEN(57),DEND(57),SOE(57),PAI(57),VIS(57),VISD(57),
2D(57),PS(57),DX(57),DP(57),VD(57),A(57),S(57),Q(57,65),
3DE1(57),HO(21),SUBV(65),F(65),C(2,3,65),BET(40,40),D1(57),
4PP(57),PT(57)
  X=XO $ IT=1 $ NR=5$ NW=6$ DELX=DELXO
  WRITE(6,210) C1,C2,C9,XC,X3
8 FC=PHI(X)
  IF(M.EQ.1) GO TO 40
  IF(IT-1) 10, 10, 15
10 X1=X $ X=X+DELX $ GO TO 11
15 FC2=FC $ DFC=(FC2-FC1)/(X2-X1)
  DELX=-FC/DFC
  IF(ABS(FC)-CONV) 25, 25, 20
20 X1=X $ X=X+DELX
11 FC1=FC $ X2=X $ IF(IT-NIT) 22, 22, 25
22 IT=IT+1 $ WRITE(NW,7) IT, FC, X, DELX
  IF(X.GE.XMAX) GO TO 25
  IF(X.LT.XMIN) GO TO 25
  GO TO 8
40 FC=PHI(X)
  TDC=-96.0*U/X**3
  DEX=-FC/TDC
  IF(ABS(FC)-CONV) 25, 25, 42

```



```

42 IF(IT.LE.3) 50,51
50 FA=IT $ GO TO 52
51 FA=3.0
52 DELX=FA*DEX/3.0
  X=X+DELX $ IF(IT-NIT) 43, 43, 25
43 IT=IT+1 $ WRITE(NW,7) IT,FC,X,DELX
  IF(X.GT.XMAX) GO TO 25
  IF(X.LT.XMIN) GO TO 25
  GO TO 40
25 WRITE(NW,7) IT, FC, X, DELX
  RETURN
210 FORMAT(5E12.5)
  7 FORMAT(5H IT=, I5, 4H FC=, E12.5, 5H X=, E12.5,
    X5H SX=, E12.5)
  END
' END OF RECORD

```



## REFERENCES

1. A. N. Grubin and I. E. Vinogradova (1949), Central Scientific Research Institute for Technology and Mechanical Engineering, Book No. 30, Moscow, (D.S.I.R. Translation No. 337).
2. D. Dowson and G. R. Higginson, "The Effect of Material Properties on the Lubrication of Elastic Rollers", *Journal of Mechanical Engineering Science*, Vol. 2, No. 3, p. 188.
3. H. S. Cheng and B. Sternlicht, "A Numerical Solution for the Pressure, Temperature, Film Thickness Between Two Infinitely Long Lubricated Rolling and Sliding Cylinders, Under Heavy Loads", ASME Transaction, Journal of Basic Engineering, Vol. 87, 1965, pp. 695-707.
4. H. S. Cheng, "A Refined Solution to the Thermal-Elastohydrodynamic Lubrication of Rolling and Sliding Cylinders", *Transactions of the American Society of Lubrication Engineers*, Vol. 8, 1965, pp. 397-410.
5. D. Dowson and A. V. Whitaker, "A Numerical Procedure for the Solution of Elastohydrodynamic Problem of Rolling and Sliding Contacts Lubricated by Newtonian Fluid", *Proceedings of the Institute of Mechanical Engineers*, Vol. 180, Part 3, Series B, 1965, pp. 57-71.
6. K. M. Lee and H. S. Cheng, "The Pressure and Deformation Profiles ~~Between Two Colliding Lubricated Cylinders~~", NASA CR-1944, 1971.
7. P. E. Fowles, "The Application of Elastohydrodynamic Theory to Individual Asperity-Asperity Collisions", *Journal of Lubrication Technology, Transaction of ASME, Series F*, Vol. 91, pp. 464-476, 1969.





POSTMASTER: If Undeliverable (Section 158  
Postal Manual) Do Not Return

*"The aeronautical and space activities of the United States shall be conducted so as to contribute . . . to the expansion of human knowledge of phenomena in the atmosphere and space. The Administration shall provide for the widest practicable and appropriate dissemination of information concerning its activities and the results thereof."*

—NATIONAL AERONAUTICS AND SPACE ACT OF 1958

## NASA SCIENTIFIC AND TECHNICAL PUBLICATIONS

**TECHNICAL REPORTS:** Scientific and technical information considered important, complete, and a lasting contribution to existing knowledge.

**TECHNICAL NOTES:** Information less broad in scope but nevertheless of importance as a contribution to existing knowledge.

**TECHNICAL MEMORANDUMS:** Information receiving limited distribution because of preliminary data, security classification, or other reasons. Also includes conference proceedings with either limited or unlimited distribution.

**CONTRACTOR REPORTS:** Scientific and technical information generated under a NASA contract or grant and considered an important contribution to existing knowledge.

**TECHNICAL TRANSLATIONS:** Information published in a foreign language considered to merit NASA distribution in English.

**SPECIAL PUBLICATIONS:** Information derived from or of value to NASA activities. Publications include final reports of major projects, monographs, data compilations, handbooks, sourcebooks, and special bibliographies.

**TECHNOLOGY UTILIZATION PUBLICATIONS:** Information on technology used by NASA that may be of particular interest in commercial and other non-aerospace applications. Publications include Tech Briefs, Technology Utilization Reports and Technology Surveys.

*Details on the availability of these publications may be obtained from:*

**SCIENTIFIC AND TECHNICAL INFORMATION OFFICE**

**NATIONAL AERONAUTICS AND SPACE ADMINISTRATION**  
Washington, D.C. 20546